# OUTLET DISCHARGE COEFFICIENTS OF VENTILATION DUCTS

by

## ROGER GORDON KINSMAN

A thesis submitted to the Faculty of Graduate
Studies and Research in partial fulfilment
of the requirements for the degree of
MASTER OF SCIENCE

in

Agricultural Engineering

Macdonald College of
McGill University, Montreal

@ January, 1990

# OUTLET DISCHARGE COEFFICIENTS OF VENTILATION DUCTS

by

# ROGEK GORDON KINSMAN

Macdonald College of
McGill University,
Montreal

**@**1990

#### **ABSTRACT**

Discharge coefficients are an important parameter in the prediction of the air displacement performance of ventilation outlets and in the design of ventilation ducts.

Discharge coefficients of a wooden ventilation duct 8.54 metres in length and of a constant 0.17 m<sup>2</sup> cross sectional area were measured. Four different outlet shapes and 3 aperture ratios of each shape were tested. A split plot experimental design was used to evaluate the effect of outlet shape, outlet size, and distance from the fan on discharge coefficient. The relationship between duct performance characteristics and discharge coefficient was examined. A mathematical equation to predict the discharge coefficient was developed and tested.

Discharge coefficient values measured ranged from 0.19 to 1.25 depending on the aperture ratio and distance from the fan. Outlet shape had no significant effect. The apparent effects of aperture ratio and size are due to the effects of head ratio. The equation predicting the discharge coefficient had a maximum error of 5 percent for the aperture ratios of 0.5 and 1.0, and 15 percent at an aperture ratio of 1.5.

#### RESUME

Les coefficients de débit sont un paramêtre important dans la conception des conduits perforés de ventilation et pour prédire la répartition de l'air aux bouches de sortie.

Les coefficients de débit d'un conduit de ventilation en bois d'une longueur de 8.54 mêtres et d'une surface transversale de 0.17 m² ont été mesurés. Quatre formes différentes d'ouverture et trois ratios d'ouverture ont été testés pour chacune des formes. Un design expérimental statistique "split plot" a été utilisé pour évaluer l'effet de la forme de l'ouverture, de la dimension de l'ouverture et de la distance à partir du ventilateur sur le coefficient de débit. La relation entre la performance du conduit et le coefficient de débit a été examinée. Une équation mathématique prédisant le coefficient de débit a été développée et testée.

Les valeurs du coefficient de débit se situaient entre 0.19 et 1.25 selon le ratio d'ouverture et la distance à partir du ventilateur. La forme de l'ouverture n'a eu aucun effet significatif. L'effet apparent du ratio et de la dimension de l'ouverture est causé par l'effet du ratio de charge de pression. L'équation prédisant le coefficient de débit avait une erreur maximum de cinq pourcent pour les ratios d'ouverture de 0.5 et 1.0, et de 15 poucent pour un ratio d'ouverture de 1.5.

## **ACKNOWLEDGEMENTS**

I sincerely express my gratitude to Dr. S.F. Barrington for her assistance and guidance throughout this project.

I would also like to thank Mr. Ian MacKinnon for his assistance in constructing the experimental equipment and calibrating the instruments, and Ms. Yan Fu for her assistance in the mathematical analysis of the duct.

I would like to acknowledge the financial support of the Québec Ministry of Agriculture, Food and Fisheries as well as the Natural Sciences and Engineering Research Council of Canada.

# TABLE OF CONTENTS

PAGE
Abstract
Résumé ii
Acknowledgements
Table of Contents
List of Figures
List of Tables
1.0 Introduction
1.1 Objectives
1.2 Scope
2.0 Literature Review
2.1 Historical Perspective
2.2 Factors Affecting Pischarge Coefficients 6
2.3 Evaluation of Discharge Coefficients
2.4 Mathematical Modelling of Discharge Coefficients 11
3.0 Theory
4.0 Equipment and Procedure
4.1 Equipment
4.2 Procedure
4.3 Statistical Analysis
5.0 Results and Discussion
6.0 Conclusions
7.0 Recommendations for Further Reasearch
8.0 References

9.0 Appendices	• • • •	• • • •	• • • • • • • • •	• • • • • • • • •	72
9.A.1 Experimental	data .	• • • •		• • • • • • • •	72
9.A.2 Mean Values				• • • • • • • •	85
9.B Statistical Ana	veie				<u> </u>

# LIST OF FIGURES

FIGURE	TITLE	PAGE
3.1 :	The mathematical model	16
3.2a :	Zero axial momentum at the outlet	20
3.2b:	Streamline flow at the outlet	20
4.1 :	The experimental duct	24
5.1 :	Pressure curves for aperture ratio = 0.5	30
5.2 :	Pressure curves for aperture ratio = 1.0	31
5.3 :	Pressure curves for aperture ratio = 1.5	32
5.4 :	Outlet velocity curves for aperture ratio = 0.5	33
5.5 :	Outlet velocity curves for aperture ratio = 1.0	34
5.6 :	Outlet velocity curves for aperture ratio = 1.5	35
5.7 :	Head ratio curves for aperture ratio = 0.5	36
5.8 :	Head ratio curves for aperture ratio = 1.0	37
5.9 :	Head ratio curves for aperture ratio = 1.5	38
5.10:	Discharge coefficients for aperture ratio = 0.5	41
5.11 :	Discharge coefficients for aperture ratio = 1.0	42
5.12 :	Discharge coefficients for aperture ratio = 1.5	43
5.13 :	Discharge coefficient vs. head ratio:	47
5.13 :	Discharge coefficient vs. head ratio:	48
5.14:	Discharge coefficient vs. head ratio:	49
5.16 :	Discharge coefficient vs. duct Reynolds number: Aperture ratio =0.5	50
5.17:	Discharge coefficient vs. duct Reynolds number: Aperture ratio =1.0	51

FIGURE	TITLE	PAGE
5.18:	Discharge coefficient vs. duct Reynolds number: Aperture ratio =1.5	52
5.19:	Discharge coefficient vs. outlet Reynolds number: Aperture ratio =0.5	53
5.20:	Discharge coefficient vs. outlet Reynolds number:  Aperture ratio =1.0	54
5.21 :	Discharge coefficient vs. outlet Roynolds number: Aperture ratio =1.5	55
5.22:	Head ratio curves (averaged over $\theta$ for all shapes)	58
5.23:	Equation 3.16 vs. the data	60
5.24:	The duct velocity model	61
5.25:	The duct energy model	62

# LIST OF TABLES

TABLE	TITLE	PAGE
4.1 :	Size - Shape combinations	25
5.1 :	Duct inflow vs. duct discharge	40
5.2 :	Summary of statistical analysis	44
5.3 :	r <sup>2</sup> values for the linear regression analyses	46
A1 to A12	: The experimental data for each shape	73-84
B1 and B2	: Statistical analysis: Split plot experimental design	87

#### 1.0 INTRODUCTION

Air distribution ducts are widely used in the mechanical ventilation of agricultural structures. The purpose of these ducts is to introduce fresh air into the structure while recirculating inside air. For adequate ventilation performance the correct amount of air must be properly distributed within the structure (Hellickson and Walker, 1983). A properly designed system offers the advantages of allowing sufficient air to pass through the structure to control moisture, temperature, and airborne pollutants, and of developing acceptable patterns of airflow throughout the entire structure without creating excessive cold drafts (Leonard, 1987). To properly design an air distribution duct, it is necessary to be able to predict the air displacement performance of the system.

One problem in predicting the air displacement performance of air distribution ducts is that the actual flow rate at the outlets is often different from the potential flow rate expected as a result of the energy differential between the duct air and the room air. The coefficient of discharge of a ventilation duct outlet is the ratio of the actual volumetric flow rate to the potential volumetric flow rate. This coefficient of discharge is a means of accounting for outlet discharge based on the energy differential between the duct and room air and represents the energy losses at the outlet.

Discharge coefficients have been well defined for various types of wall and ceiling outlets (Albright 1976, 1978) but little is known of discharge coefficients of ventilation duct perforations. Mathematical models have previously been developed to determine the air displacement performance of distribution ducts. In order to apply these models, it is necessary to evaluate the discharge coefficient for each outlet along the length of the duct. The initial approach to

evaluating discharge coefficients of air distribution duct perforations has been to assume that the perforations are similar to a sharp edge orifice plate and have a constant discharge coefficient along the length of the duct (Steele and Shove, 1969). However, research has demonstrated that discharge coefficient values vary under different operating conditions (Rawn et al 1960). Empirical relationships for discharge coefficient values have been developed. These relationships give good results but because they are empirically derived they may not apply to all ventilation ducts.

It is important to accurately evaluate discharge coefficient values to avoid costly errors in designing ventilation systems (Hellickson and Walker, 1983). Saunders and Albright (1984) found the discharge coefficient to be the most important factor in modelling duct air flow. It was the purpose of this study to increase our understanding of the factors that influence the discharge coefficient and to use fluid mechanics principles to find a method of predicting discharge coefficient values.

#### 1.2 OBJECTIVES

This project had the following objectives:

- 1) To determine if the outlet location along the length of the duct effects discharge coefficient values.
- 2) To determine if outlet geometry (shape and size), has an effect on the discharge coefficients of ventilation ducts.
- 3) To establish the relationship between the duct performance characteristics and the coefficient of discharge. Performance characteristics include duct static pressure, duct velocity, outlet velocity, and outlet discharge angle.

4) To develop and test an equation that predicts discharge coefficient values for ventilation ducts.

#### 1.1 SCOPE

This study involved the use of a wooden duct of fixed length and constant cross sectional area. Four different shapes of outlets commonly used, and three aperture ratios of each shape were examined. Each combination of outlet shape and size was installed on the duct and tested at 100% fan speed. The type of duct tested was of typical dimensions used in agricultural structures. One fan speed, one duct length to diameter ratio, one duct sidewall thickness, and one type of duct was used. Further experiments, varying these parameters, are required to determine if the results of this study are universally applicable to ventilation ducts.

#### 2.0 LITERATURE REVIEW

Accurate mathematical analysis of air distribution duct performance is difficult because the actual outlet velocities are usually not equivalent to the outlet velocity that would be theoretically expected (Esmay and Dixon, 1986). One reason for this is that air flowing through a small opening will suffer the effects of a vena contracta resulting in an effective flow area less than the actual area of the outlet. Another reason is that the edge of the outlet, the viscosity of the air passing through the outlet, and the contraction of the jet, all create friction losses in the flow (Hellickson and Walker, 1983). The discharge coefficient is the product of the coefficient of contraction and the coefficient of velocity which account for the contraction of the air and the friction losses at the outlet, respectively (Hellickson and Walker, 1983).

To accurately apply the fundamental equations of fluid mechanics to air distribution duct performance it is necessary to accurately determine the discharge coefficient values of the outlets. Haerter (1963) demonstrates that the fundamental equations required to predict ventilation duct performance are the conservation of mass and the conservation of momentum. The equations associated with these principles make several assumptions that may or may not apply at the outlets of a particular system. These assumptions include (Roberson and Crowe, 1980):

- i) Steady state conditions.
- ii) Air flows over the entire area of the outlet.
- iii) No friction losses at the outlet.
- iv) Constant and even velocity profiles in the duct.

Since distribution duct systems may be assumed to operate under steady state conditions the discharge coefficient should correct for the other 3 assumptions.

Hellickson and Walker (1983) pointed out that the proper evaluation of the discharge coefficient is very important otherwise substantial errors can result in the design of ventilation systems. Smith et al. (1986), and Saunders and Albright (1984) clearly demonstrate that the design of systems similar to ventilation ducts is very sensitive to the value of discharge coefficient chosen.

The mathematical analysis of several types of systems that are governed by the same principles as wooden ventilation ducts are available in the literature. These include various manifold systems and other types of ventilation ducts, as well as ventilation inlets. A manifold is a device for distributing liquid or gas in which the fluid is conveyed through a main tube and ejected through a series of side ports (Denn, 1980). Ventilation distribution ducts are very similar to the various types of manifolds examined in the literature. These manifolds include pipe burners, sewage diffusers, and water distribution systems. Other types of ventilation ducts are perforated corrugated tubing, and perforated polyethylene tubing. Ventilation inlets examined in the literature include perimeter slotted inlets and centre ceiling slotted inlets.

#### 2.1 HISTORICAL PERSPECTIVE

Research, and mathematical analyses, that can be applied to the air flow distribution from ventilation ducts began in late 1800's. Howland (1953) cites a paper from 1865 giving rules for the uniform discharge from water distribution pipes. McNown (1954) states that investigators in several different fields have been conducting studies on manifold flow since the turn of the century. Up until

the 1950's research was focused on the even distribution from water distribution pipelines and gas burners. In the 1950's research began to apply these theoretical flow equations to ventilation ducts. Researchers began to study ventilation ducts that are specific to agricultural structures in the 1960's. In the 1970's and 1980's further research has been conducted on polyethylene ventilation ducts.

#### 2.2 FACTORS AFFECTING DISCHARGE COEFFICIENTS

Several factors have been found to affect the magnitude of the discharge coefficient including the Reynolds number, outlet geometry, and the ratio of pressure head to total head. The Reynolds number is a dimensionless parameter which is the ratio of the viscous forces to the inertial forces of the fluid. By definition Reynolds number is:

Re = Dh 
$$\rho$$
 V /  $\nu$  = f (Dh,  $\rho$ , V,  $T_{abe}$ ) ............ (2.1)

where: Dh = the hydraulic diameter, m

 $\rho$  = the fluid density, kg/m<sup>3</sup>

V = the fluid velocity, m/s

v =the dynamic viscosity,  $N s/m^2$ , and

 $T_{abs}$  = the absolute temperature, °K.

Lichtarowitz et al. (1965) cites a paper which states that the discharge coefficient is essentially a function of Reynolds number and the ratio of orifice diameter to pipe diameter. In tests involving an aviation kerosene distributor, Spikes and Pennington (1959) found that the effect of Reynolds number on

discharge coefficient decreases as the Reynolds number increases. Trengrouse (1970) found that discharge coefficient is a function of Reynolds number by dimensional analysis but offered little experimental evidence. Albright (1976) determined that the discharge coefficient of a hinged baffle slotted inlet may be slightly dependant on Reynolds number. Trengrouse (1970) found that the effect of temperature on the discharge coefficient of air ducts was negligible in the tested range of 15 °C to 150 °C. From equation 2.1, this would suggest that for a given ventilation system operating under normal conditions, where Dh, ρ, and air temperature are essentially constant, Reynolds number effects are due solely to the velocity parameter. Howland (1953) and Dittrich and Graves (in Bailey, 1975) found that pipe velocity was the most important factor affecting the discharge coefficient of a water distribution pipe.

The geometry of an outlet orifice, or its shape and size, as well as the wall thickness contribute to the friction losses in terms of wall surface exposed to flow (Spikes and Pennington, 1959). Bailey (1975) cites a paper stating that the discharge coefficient is a function of orifice size in relation to pipe diameter and wall thickness. Howland (1953) found that the orifice geometry had an effect on the discharge coefficient but that this effect was not as important as the effect of pipe velocity. Bailey (1975) cites a paper by Dittrich and Graves that also found that the effects of orifice size and wall thickness on discharge coefficient were not as important as the effects pipe velocity. Trengrouse (1970) found that varying the ratio of total outlet area to pipe cross sectional area of small holes (9.5 to 13 mm in diameter) in a small pipe (50mm in diameter) had no effect on the discharge coefficient and that pipe walls thinner than 1.6mm had no effect on the discharge coefficient.

Several researchers have found that the discharge coefficient of manifold outlets changes as the pressure head becomes a larger part of the total head. The ratio of pressure head to the total head (pressure head plus the velocity head) is commonly referred to in the literature as the head ratio (HR). Enger and Levy (1929), Rawn et al. (1960), and Davis et al. (1980), all expressed the discharge coefficient in the form of:

where: HR = the ratio of pressure head to total head

 $Cd_{max}$  = the Cd measured where HR=1.0 (the dead end of the manifold).

Bailey (1975) found that when the pressure head was much greater than the velocity head, the discharge coefficient tended towards a maximum value, and when the velocity head was much greater than the pressure head he found that the discharge coefficient tended towards zero. Kincaid and Kemper (1982) found the discharge coefficient of irrigation manifolds to vary with the head ratio in the following form:

$$Cd_{x} = 1 - a/(b+HR) \qquad (2.3)$$

where: Cd<sub>x</sub> = the discharge coefficient at a point X metres from the end of the duct.

a,b = regression parameters

Ramamurthy and Satish (1987) found discharge coefficient to be a function of the head ratio in quadratic form as:

No explanations were offered by any of the authors of equations 2.2 to 2.4 concerning the relationship between discharge coefficient and head ratio.

### 2.3 EVALUATION OF DISCHARGE COEFFICIENTS

Several different values have been assigned to the discharge coefficient of manifold orifices. Many researchers have achieved good experimental results simply by assuming that the discharge coefficient of a manifold orifice is equal to that of a sharp edge orifice plate. They have also assumed the discharge coefficient to be constant over the length of the manifold. Koestel and Young (1951) assumed that the discharge coefficient of a long slot used for air distribution was equal to 0.61. Steele and Shove (1969) suggest that in designing ventilation ducts a discharge coefficient of 0.60 be used for the entire length of the duct. Allen (1974) basically assumed that the discharge coefficient of 12mm x 45mm slots in a ventilation duct was equal to 1.0. Saunders and Albright (1984) used a value of 0.64 for the entire length of a polyethylene ventilation duct. Smith et al. (1986) assumed that the discharge coefficient of gated irrigation pipe was equal to 0.65 and remained constant with distance along the pipe.

Several researchers found that the discharge coefficient varied over the length of a manifold. These researchers found that discharge coefficient reached a maximum value, that of sharp edged orifice plate, at the end of the manifold and decreased along the length of the pipe. Rawn et al. (1960), French (1972),

Bailey (1975), Davis et al. (1980), as well as Kincaid and Kemper (1982), all stated that the discharge coefficient varied between zero and that of a sharp edge orifice plate, depending on the head ratio. The maximum value of discharge coefficient expected by these authors ranged from 0.61 to 0.65.

Several authors have experimentally evaluated the discharge coefficient of different types of manifold systems with a wide range of results. Enger and Levy (1929) worked with a water distribution manifold with lateral tubes at 90 degree angles to the pipe. The measured discharge coefficient values varied between 0.69 and 0.75 over the length of the pipe. Ramamurthy and Satish (1987) found the discharge coefficient of a similar system to vary from zero to 0.80. Van't Woudt (1964) found the discharge coefficient of a water distribution pipe to be 0.72 ±7% over the length of the pipe. Spikes and Pennington (1959) found the discharge coefficient of 3.175mm holes on a 50mm copper tube to range between 0.63 and 0.66.

The discharge coefficient values of other types of ventilation inlets are well defined in the literature. Albright (1976) measured the discharge coefficient values of hinged, baffle slotted inlets that were not subjected to any abrupt change in flow direction. The discharge coefficient value of this type of inlet was found to vary between 0.721 and 0.862 depending on the baffle angle. Albright (1978) found that varying the baffle width, slot width, and inlet throat width of a centre ceiling slotted inlet produced a discharge coefficient ranging from 0.20 to 0.80. Smith and Hazen (1966) measured the discharge coefficient of an L-shaped slot inlet, where the air jet had to turn over 90 degrees at the opening. Based on the average air velocity, a value of about 0.40 was measured for the discharge coefficient.

### 2.4 MATHEMATICAL MODELLING OF DISCHARGE COEFFICIENTS

In order to mathematically model discharge coefficients the flow characteristics in the duct and at the outlet must be modelled. Three different approaches to the mathematical modelling of manifold flow can be found in the literature: the approximation of a uniformly porous wall, outlet by outlet iteration, and the approximation of a long slot. Olson (1949) derived the differential equations for flow in a long unbranched pipe with uniformly spaced outlets by assuming it to be similar to a pipe with a uniformly porous wall. There were no experimental data to prove the theory. Bajura (1971), Ramirez-Guzman and Manges (1971), as well as Ramamurthy and Satish (1987) used similar assumptions and had good experimental results in modelling the discharge from water distribution pipes.

The technique of starting at the downstream end, where the boundary conditions are known, and applying the governing equations outlet by outlet along the manifold, was used by Keller (1949) to get even distribution of fuel from gas burners. Kincaid and Kemper (1982) and Smith (1988) used this method to successfully model the flow of water from distribution pipes. Davis et al. (1980), modelling the flow from corrugated tubing, and Saunders and Albright (1984), modelling the flow from perforated polyethylene tubing, approximated flow performance to within 25% and 10%, respectively, with this method.

Enger and Levy (1929) found it convenient to assume that air distribution through a large number of holes is equivalent to the flow through a long slot. Keller (1949) states that where the equations can be integrated it is preferable to treat the openings as a continuous slot. Koestel and Young (1951)

developed the equations for flow through a long slot. Haerter (1963), in a review of papers, found the approximation of a long slot to be the most desirable method to use. Barrington and MacKinnon (1990) successfully used this method to develop and test models of duct velocity and energy in wooden ventilation ducts.

The discharge coefficient is usually evaluated in the literature as the ratio of the measured outlet velocity to the potential or theoretical outlet velocity. Koestel and Young (1951), Howland (1953), Spikes and Pennington (1959), Bailey (1975), Albright (1976), and Saunders and Albright (1984), state that:

$$V_{\text{notential}} = (2 \text{ g h})^{1/2} \qquad \dots \qquad (2.5)$$

where:  $V_{potential}$  = the expected theoretical velocity, m/s

g = the acceleration of gravity, m/s<sup>2</sup>, and

h = the pressure head, m.

This equation applies the Bernoulli energy equation to the outlet, assuming that the fluid discharges at a 90 degree angle, that the air follows definite streamlines, and that the entire pressure head is converted to velocity at the outlet. Rawn et al. (1960) assumes that the total head, the pressure head plus the velocity head, is converted to velocity at the outlet. This suggests that:

$$V_{potential} = (2 g e)^{1/2} \dots (2.6)$$

where: e = the total energy head, m.

Davis et al. (1980) points out that including the total energy head term accounts for the flow leaving the orifice at an angle other than 90 degrees. Other authors who have used this approach include Kriess (1945), French (1972), and Barrington and MacKinnon (1990).

Evaluating the duct energy head, and thus the discharge coefficient, is difficult for two reasons. The first being that the air flow near the duct wall differs from the average duct velocity. This difference depends on the location along the length of the duct (Haerter, 1963). The second is that the energy per unit mass given by the mean velocity squared is not the average of the sum of the velocities squared over the duct cross section (Streeter and Wylie, 1981). These inaccuracies are due to a variable velocity profile over the cross sectional area of the duct.

The inaccuracies that the variable velocity profile creates have been approached in several different ways in the literature. Soucek and Zelnick (1945) mention the effects of the variable velocity profile but ignore them in their analysis of lock manifolds. Escobar (1954) states that a correction factor is necessary because the lateral discharge comes from a region of low velocity, where the kinetic energy relative to the remaining flow is less than average. Haerter (1963) states that the lateral discharge comes from a region in which the velocity may be higher or lower than the remaining flow depending on location along the duct.

Several authors have used a correction factor to account for the variable velocity profile. Berlamont and Van der Beken (1973) assumed a constant correction factor of 1.075 along the length of the pipe. Smith et al. (1986) and

Smith (1988) found that assuming a constant correction factor of 1.1 along the length of a pipe produced good results with their model. Haerter (1963) and Barrington and MacKinnon (1990) found that the correction factor varied along the length of the duct. Barrington and MacKinnon (1990) found that depending on aperture ratio, the correction factor ranged from about 2 to 20 for a wooden ventilation duct and applied to both momentum and kinetic energies.

#### 3.0 THEORY

A ventilation duct operating under steady state conditions will function according to the laws of conservation of mass and conservation of momentum. If the air flows through a series of equally spaced orifices, then it can be assumed to be distributed from a long slot (figure 3.1). The distance X is measured from the end of the duct where X=0. It is also assumed that the duct will demonstrate pressure regain, where pressure inside the duct will increase with distance from the fan as the air decelerates due to the flow out the side slot. The mathematical analysis of the duct is simplified if the duct is assumed to operate under steady state conditions. For a duct with a long slot outlet, the ratio of the total outlet area to the cross sectional area of the duct, or the aperture ratio ( $\theta$ ), can be expressed as:

A =the duct cross sectional area,  $m^2$ .

The outlet slot area for any increment of length dX would be:

Ao = 
$$(\theta \text{ A dX}) / L \dots (3.2)$$
  
where: Ao = the outlet slot area over dX, m<sup>2</sup>

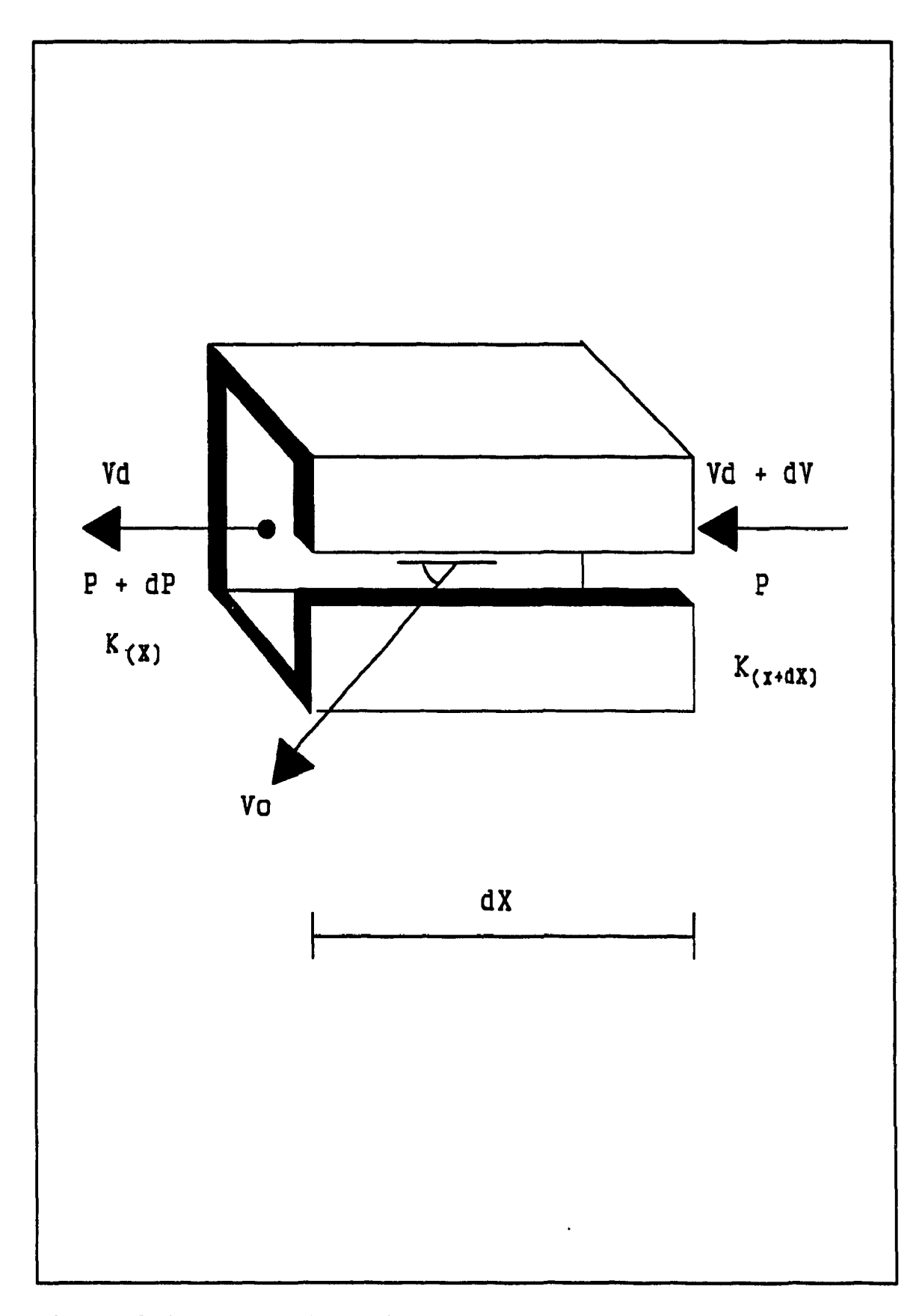


Figure 3.1 The mathematical model

and the volumetric flow rate through an increment of length dX would be:

The law of conservation of mass applied to the section of duct in figure 3.1 states that the mass flow at a point X equals the mass flow at a point X+dX minus the mass flow through the outlet over dX, or:

$$\rho AV = \rho A(V+dV) - h\rho VodX \dots (3.4)$$
 where: 
$$\rho = \text{the density of air, kg/m}^3$$
 
$$Vo = \text{the average outlet velocity, m/s}$$

or rearranging terms and substituting terms from equation 3.1:

The law of conservation of linear momentum applied to the section of figure 3.1 states that the momentum of the air at a point X equals the momentum of the air at a point X+dX minus the momentum lost to friction, and minus the momentum of the air discharged over dX:

$$A(P+dP) + AK\rho V^2 = AP + AK\rho (V+dV)^2 - \frac{fA\rho V^2}{2Dh} dX - \rho QodV \dots (3.6)$$

where: K = energy correction factor, dimensionless

f = friction factor, dimensionless, and

Dh = duct hydraulic diameter, m.

Rearranging terms, and considering equations 3.3 and 3.5, the momentum equation becomes:

$$dP + K_{(X)}V^{2} - K_{(X+dX)}(V+dV)^{2} + \frac{fdXV^{2}}{2Dh} + V_{potential}dVCd = 0 ... (3.7)$$

The energy correction factor, K, is introduced to express the duct air momentum in terms of the mean duct air velocity. The energy correction factor adjusts for the restrictive assumption of a uniform duct velocity profile and can be expressed as the ratio of the actual momentum to the momentum computed from the average duct velocity (Barrington and MacKinnon 1990). The energy correction factor accounts for the variable duct velocity profile at any point along the length of the duct (Haerter, 1963, Barrington and MacKinnon, 1990).

This correction factor can also account for assumptions required in calculating the potential energy of the air at the outlet. The potential energy of the air at the outlet can be evaluated by one of two assumptions (Denn, 1980). The first is to assume that the outlet velocity vector is perpendicular to the plane of the side port and contains no axial momentum (figure 3.2a). Using the momentum equation to calculate the duct kinetic energy at the outlet under the conditions illustrated by figure 3.2a, yields;

$$\mathbf{E} = \frac{\mathbf{P}}{\rho} + \mathbf{V}^2$$

where: E =the duct air energy that can potentially be converted to outlet velocity, or  $V^2_{potential}$ ,  $m^2/s^2$ .

The second assumption is that the flow is streamlined so that there is no mixing of the duct air and the outlet air (figure 3.2b). This streamline condition is described by the Bernoulli equation and applies to the control volume ABCD of figure 3.2b so that;

$$\mathbf{E} = \mathbf{\underline{2P}} + \mathbf{V^2}$$

Each of the two estimates involves highly restrictive assumptions and are not accurate for all ventilation systems. Considered together these two assumptions may be combined in a more appropriate expression (Denn, 1980);

With the use of this expression the correction factor K, now becomes a correction factor for both the momentum and the energy of the air in the duct (Barrington and MacKinnon, 1990).

Under ideal conditions all of the kinetic energy would be converted to velocity at the outlet so;

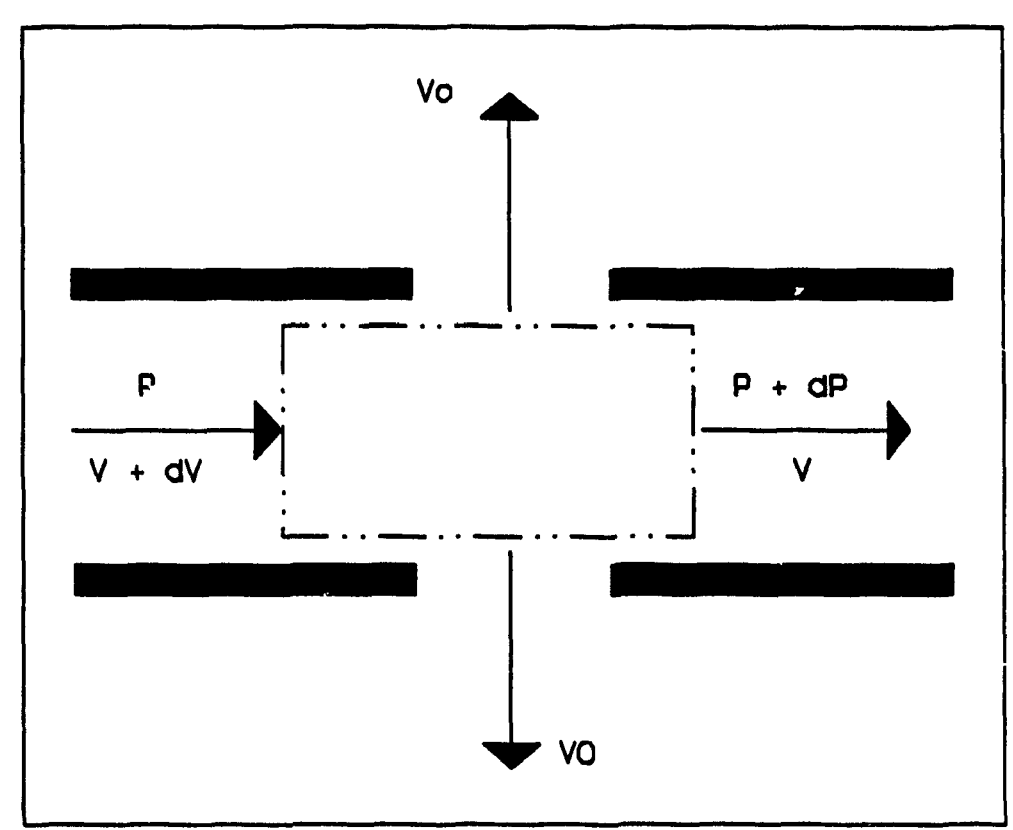


Figure 3.2a Zero axial momentum at the outlet

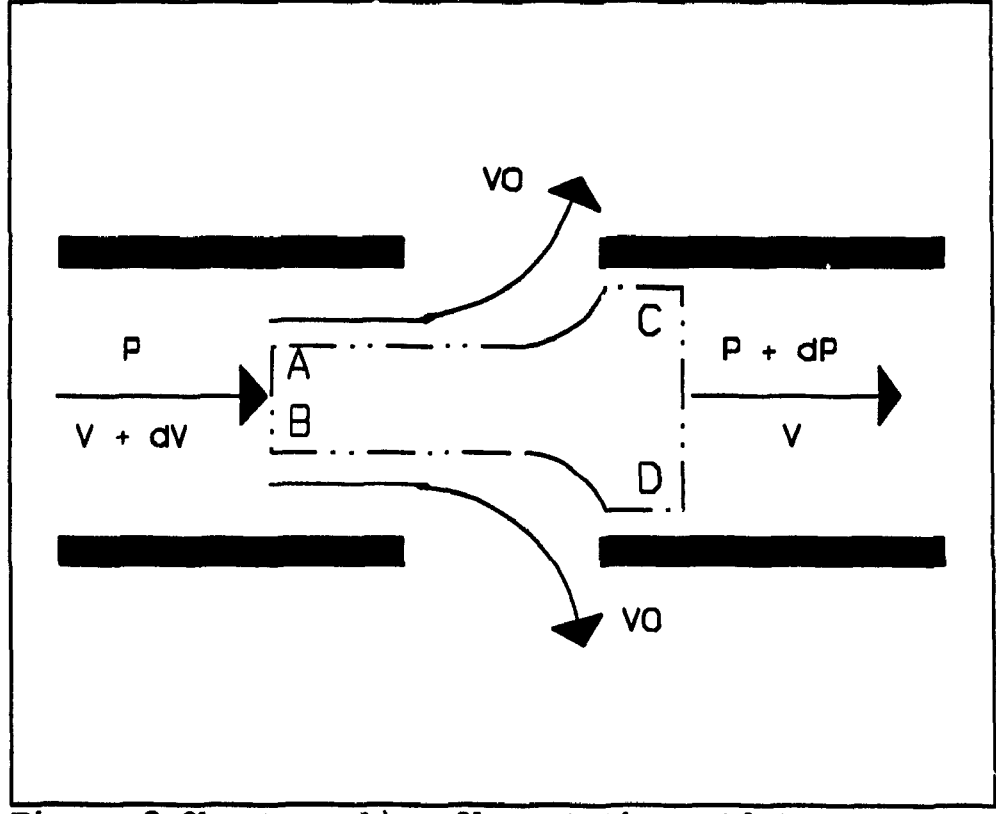


Figure 3.2b streamline flow at the outlet

## where: $E^{1/2}$ is calculated from equation 3.8

and therefore, the discharge coefficient can be described in terms of the duct energy as:

and;

where:  $Vo_x = Vo$  at any distance X, m/s

 $Cd_x = Cd$  at any distance X, dimensionless.

From equation 3.10, equation 3.5 can be written;

$$dV = ((\theta \ Cd \ E^{1/2})/L) \ dX \quad \dots \qquad (3.12)$$

Barrington and MacKinnon (1990) developed and tested models for duct velocity where;

$$V = Ho (X/L) + (Vl - Ho)(X^2/L^2) \dots (3.13)$$

where: V = average duct velocity, m/s

Ho = head at X=0 ( $\theta$  Vo at X=0), m/s

V1 = the average duct velocity at the fan, m/s

and thus;

$$dV = (Ho/L) dX + 2(V1 - Ho)(X/L^2) dX \dots (3.14)$$

Equating equations 3.12 and 3.14 yields;

from which;

$$Cd_x = [Ho + 2(Vl - Ho)(X/L)] / E^{1/2} \dots (3.16)$$

Barrington and MacKinnon (1990) also developed a model for the energy term of equation 3.8 in which;

$$E = (F/D_h) \int (V^2/2) dX + V^2/4 + VE_o^{1/2} + E_o \dots (3.17)$$

where: V is calculated from equation 3.13

$$E_{\bullet}=E$$
 at  $X=0$ 

#### 4.0 EQUIPMENT AND PROCEDURE

#### 4.1 EQUIPMENT

The experiment was conducted using a wooden duct (figure 4.1) 8.54 metres in length having a constant cross sectional area of 0.17 m<sup>2</sup> (597mm x 292mm). The duct frame consisted of 38mm x 38mm members, enclosed on the outside by 11mm thick particle board panelling. The duct was built in three, 2.44m sections and one, 1.22m section. The sections were joined with 38mm x 10mm strapping, inside the duct. A fan at one end was joined to the duct via a reduction section. The fan was a 0.25 kw, 457 mm diameter, ACME axial model equipped with an air straightener. The fan performance curve was previously determined by Barrington and MacKinnon (1990) to be Q=1.66e-4.0185P. The reduction section tapered from 597mm x 597mm at the fan to 597mm x 292mm at the experimental duct over a distance of 1.80 metres. The fan was set in an inlet box with an inlet area of 0.26m<sup>2</sup> (508mm x 508mm) to facilitate the measurement of duct inlet velocity.

To test several different outlet geometries the sidewalls of the duct were removable to allow the installation of different shapes and sizes of outlet openings. Outlets were paired, one on each side of the duct, and spaced at a 0.61m interval for a total of 28 outlets. There were 4 different shapes and 3 different sizes of outlets tested during the experiment. The following shapes were used:

- i) Half moon oriented with the air flow
- ii) Half moon oriented against the air flow
- iii) Rectangular
- iv) Circular

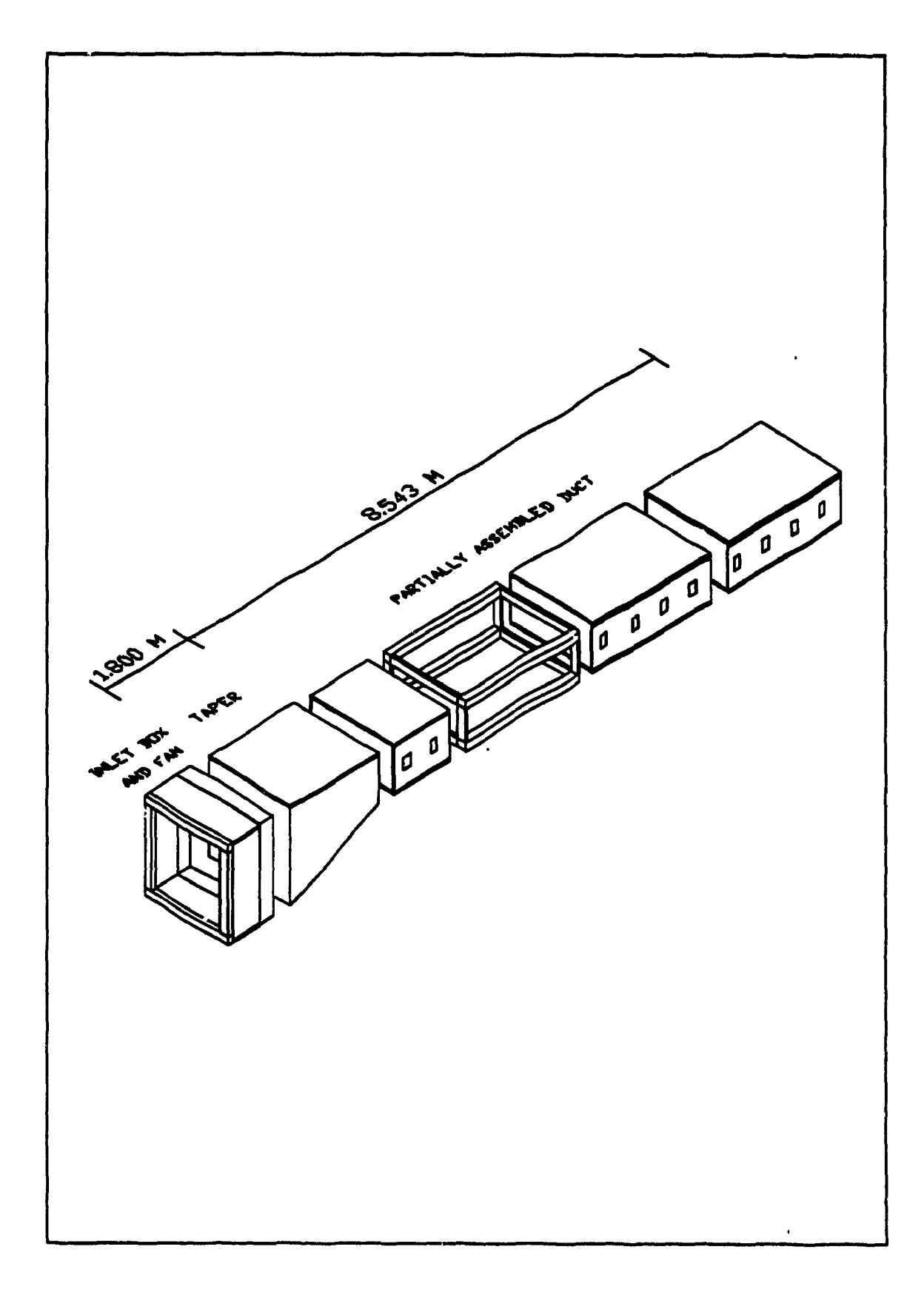


Figure 4.1 The experimental duct

To change the duct operating characteristics three different sizes of outlets were chosen to provide aperture ratios of 0.5, 1.0, and 1.5. These aperture ratios of where chosen because they have previously been found to provide a range of uniform and non-uniform distribution (Davis, 1980 and Carpenter, 1972). Each size-shape combination was cut from separate side panels to eliminate the need for an additional plate at the outlets to control size or shape. Table 4.1 contains the numbering and symbol system to be used throughout this report.

Table 4.1 Size-shape combinations

SHAPE	NO.	APERTURE RATIO		
		0.5	1.0	1.5
HALF MOON WITH AIR PLOW	1	<b>†</b>		
HALF MOON AGAINST AIR PLOW	2	$\Phi$	$\Phi$	
RECTANGULAR	3			
CIRCULAR	4	0	0	$\bigcirc$

Various instruments were used to measure air velocity, static pressure, and jet angle. Air velocity was measured using a uni-directional ALNOR compussion thermo anemometer with an accuracy of  $\pm$  3% of the indicated reading over a range of 0.1 m/s to 15 m/s. The anemometer was calibrated at

the McGill university aeronautical lab. The duct static pressure was measured using an ALNOR microtector micro manometer with an accuracy of  $\pm$  0.06 Pa over a range of 0 to 500 Pa. The pressure was tapped with bulkhead connectors placed in the top of the duct and connected to the manometer via 3mm diameter plastic tubing. Outlet air jet angle was measured using a freely rotating paper vane mounted on a protractor. The device had an accuracy of  $\pm$  2.5 degrees so the angles were read to the nearest 5 degrees.

#### **4.2 PROCEDURE**

The equipment was located in a large room to allow the formation of isothermal, free air jets. No outlet air jet was influenced by solid boundaries. The fan inlet was located in the room so that the duct air was the same temperature as the room air.

Outlet velocities were measured using the traverse method (ASHRAE, 1985) at the centre of 25mm grid squares for the half moon and rectangular shapes, and at the centre of equal sized concentric circles, along the horizontal and vertical diameters, for the circular outlets. For the aperture ratios of 0.5, 1.0, and 1.5 the outlet velocity profile was measured at no less than 4, 10, and 15 points respectively. Air flow into the duct was measured using the traverse method at the centre of 16 equal sized areas (127mm x 127mm), a pattern described in ASHRAE (1985), at the inlet box. The quantity of air flowing into the duct (m³/s) was compared to the sum of the quantity of air flowing out of the outlets to allow a check for errors. Brundrett and Vermes (1987) found that a difference of ±4.5 % was acceptable. For all air velocity measurements the anemometer was oriented to measure flows normal to the plane of the outlet, a technique also used by Saunders and Albright (1984). They showed that

measuring the air velocity normal to the plane of the outlet yields a flow equivalent to that measured parallel to the centre line of the air jet and is less subjective. All static pressure measurements were averaged over 4 readings. Outlet air jet angle was measured at the centre of the outlet opening only.

The objectives of the experiment were to test the significance of outlet location, outlet geometry, and duct operating characteristics on the discharge coefficient, as well as to test a model that predicts the discharge coefficient. To evaluate the discharge coefficient at each outlet, equation 3.10 was used. The average outlet velocity was evaluated at each outlet along one side of the duct. The duct energy head was calculated using equation 3.8. Static pressure was measured adjacent to each pair of outlets and at the end of the duct. The average duct velocity at each pair of outlets was calculated by starting at the dead end of the duct and summing the outlet volumetric flow. The kinetic energy and momentum correction factor, K, was calculated using a method similar to that of Barrington and MacKinnon (1990). Equation 3.7 was solved for  $K_{\alpha + \alpha n}$  by iteration using a computer starting at the dead end of the duct where the boundary conditions were known. At X=0,  $V_x=0$  and the value of  $K_{\infty}$ was not necessary. The discharge coefficient was initially assumed to be 1.0. Using dX = 0.61 (the outlet spacing) the average E was calculated over dX using equation 3.8 and the correlation of equation 3.10 was tested. The Cd was readjusted and the procedure repeated until the assumed Cd and V/E<sup>1/2</sup> corresponded.

## **4.3 STATISTICAL ANALYSIS**

To determine the effect of outlet location, outlet size, and outlet shape on the discharge coefficient the experiment was designed as a split plot experiment with 3 factors: outlet size (aperture ratio), outlet shape, and outlet distance from the fan. The 12 size shape combinations were randomized to the main plot units with the distance being the sub-plot unit. The experiment was repeated 3 times for an estimate of experimental error and to increase precision. To test the effect of duct performance characteristics on the discharge coefficient, the number of comparisons was reduced by combining factors into dimensionless parameters, a technique used by Davis et al. (1980). Duct velocity and outlet velocity were each combined with hydraulic diameter, air density, air kinematic viscosity, and air temperature into Reynolds number. Duct static pressure and duct air velocity were combined into the head ratio. Outlet discharge angle was considered separately.

Equation 3.16, predicting discharge coefficient values, was tested by comparing it to the experimental data. All statistical analyses were performed with the Statistical Analysis System (Statistical Analysis System Inst. Inc, 1982) on the McGill University mainframe computer.

## 5.0 RESULTS AND DISCUSSION

The discharge coefficient was evaluated from the measured duct static pressure and average outlet velocity data for the 3 aperture ratios and 4 different shapes, at 14 outlets along the length of a wooden ventilation duct. The average duct velocity, duct energy, head ratio, and duct energy correction factor were also calculated from the measured static pressure and average outlet velocity. A complete listing of the experimental data is provided in appendix A.1. Tables of mean values are provided in appendix A.2.

The static pressure, outlet velocity, and head ratio curves for each aperture ratio are presented in figures 5.1 to 5.9. From the figures it is evident that the outlet shape had very little influence on the performance of the duct. The duct static pressure demonstrated static regain and the pressure increased from the fan end towards the dead end of the duct (figures 5.1 to 5.3). The average outlet velocity was fairly constant along the length of the duct at an aperture ratio of 0.5 (figure 5.4). At aperture ratios of 1.0 and 1.5 the average outlet velocity decreased with distance from the dead end of the duct, with the exception of one outlet 8m from the dead end of the duct (figures 5.5 and 5.6). For all tests, the head ratio decreased with distance from the dead end of the duct (figures 5.7 to 5.9). The average fan capacity for aperture ratios of 0.5, 1.0 and 1.5 was 0.74 m³/s, 1.11 m³/s, and 1.34 m³/s, respectively, ±3% for all shapes.

The duct energy and momentum correction factor was calculated from equation 3.7. The correction factor ranged from 1.55 to 22.99. The measured values were very similar to those of Barrington and MacKinnon (1990), who estimated the correction factor to range from about 2 to 20. The value of the correction factor was not constant along the length of the duct, which is

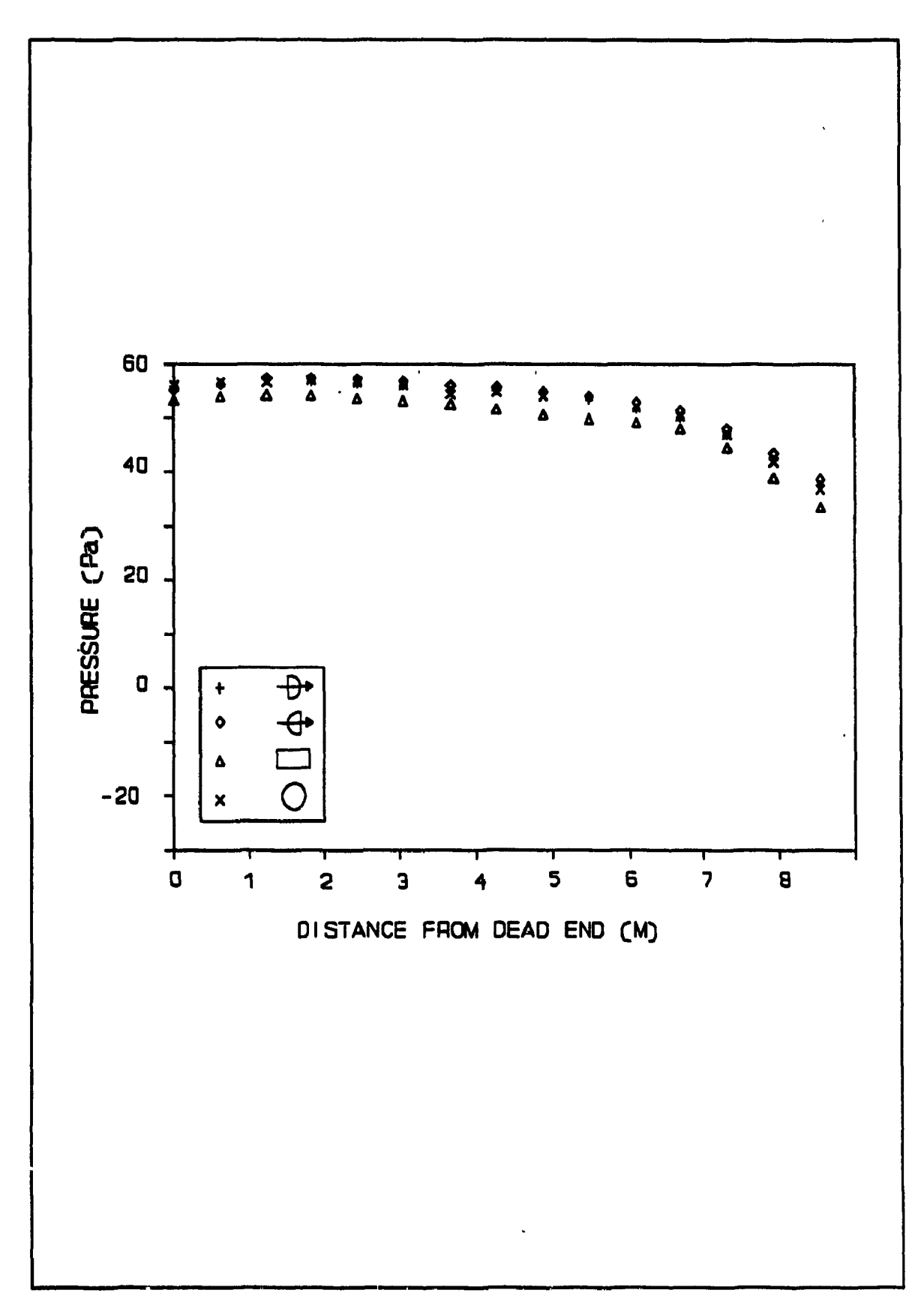


Figure 5.1 Pressure curves for Aperture ratio = 0.5

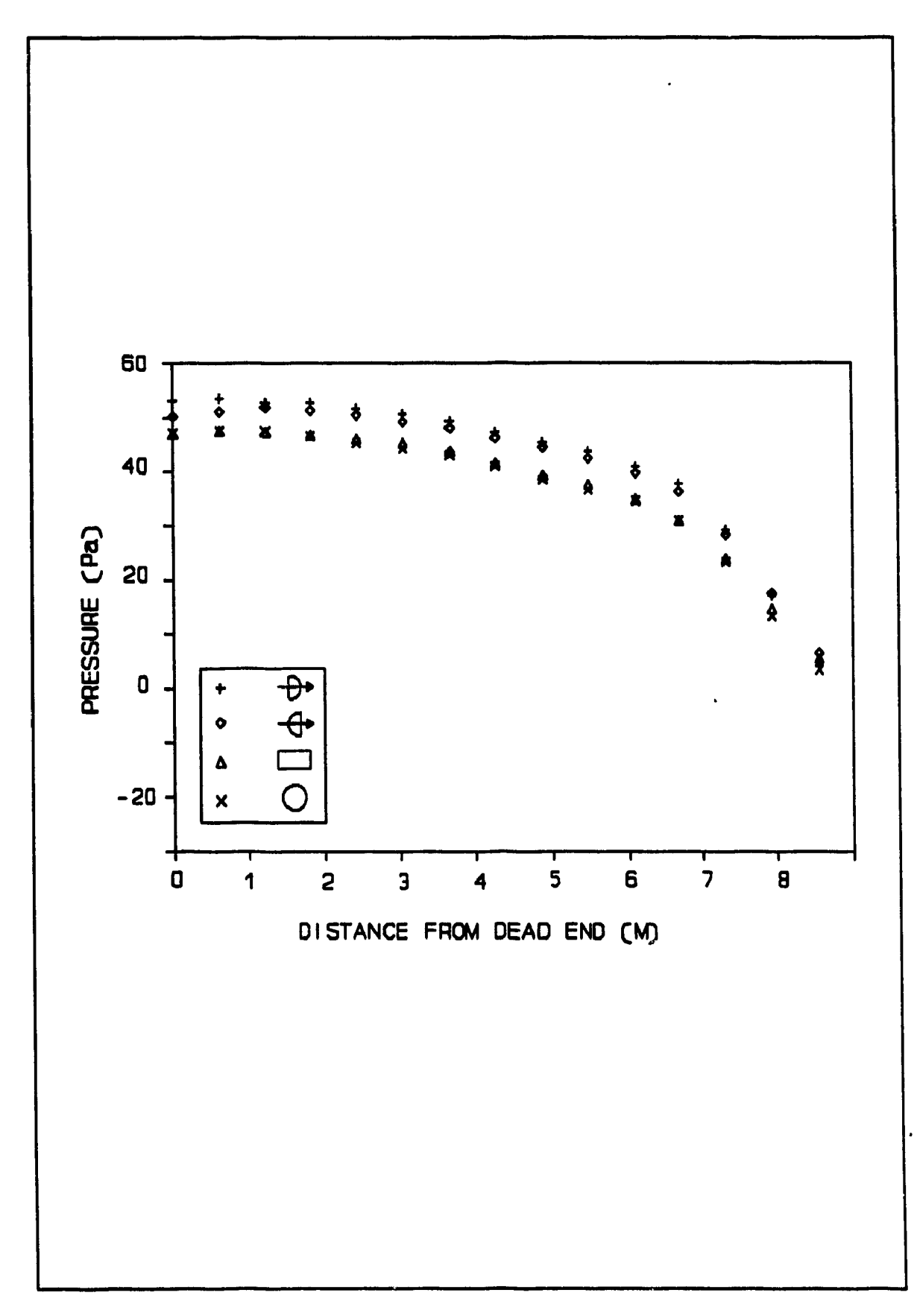


Figure 5.2 Pressure curves for aperture ratio = 1.0

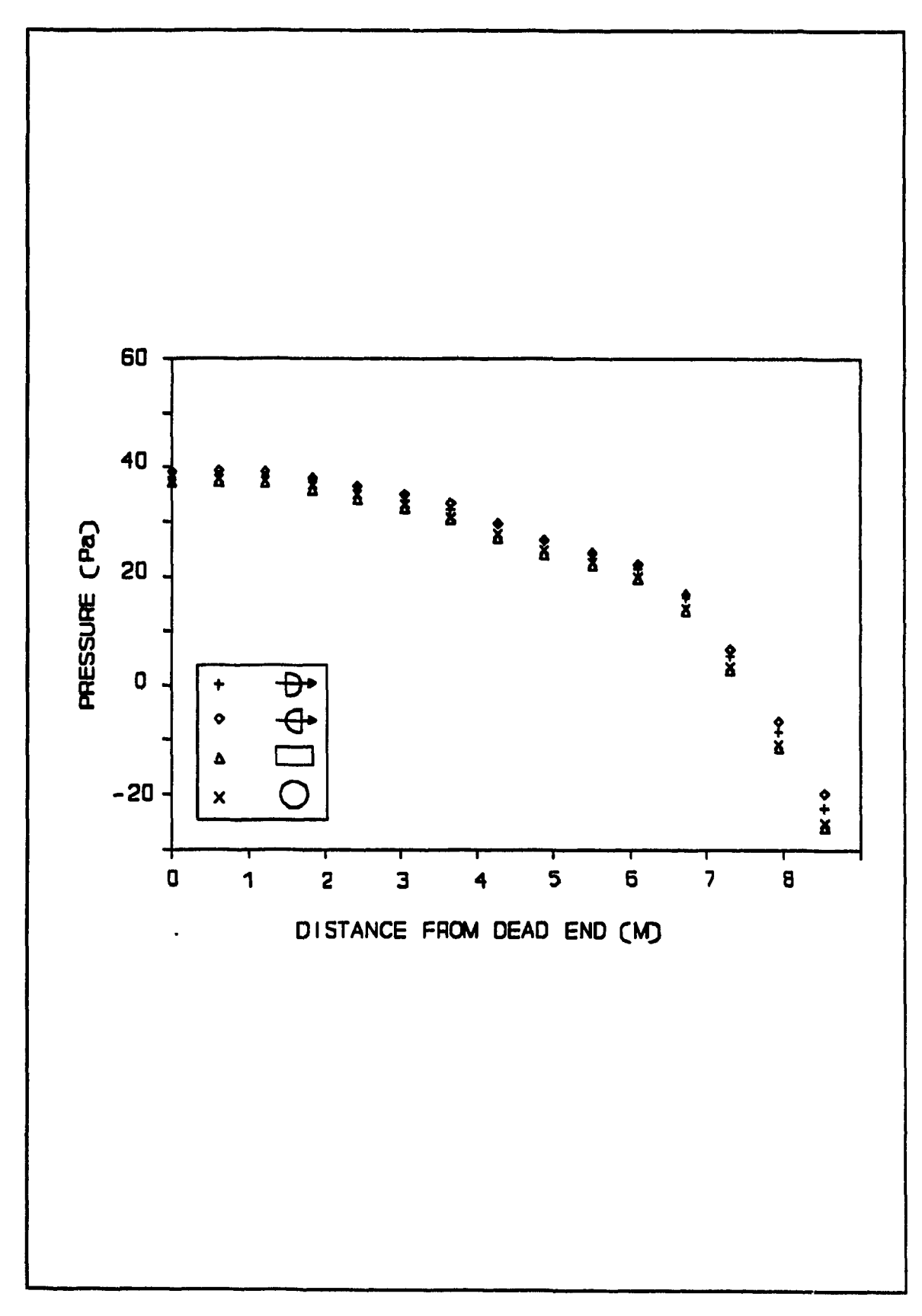


Figure 5.3 Pressure curves for aperture ratio = 1.5

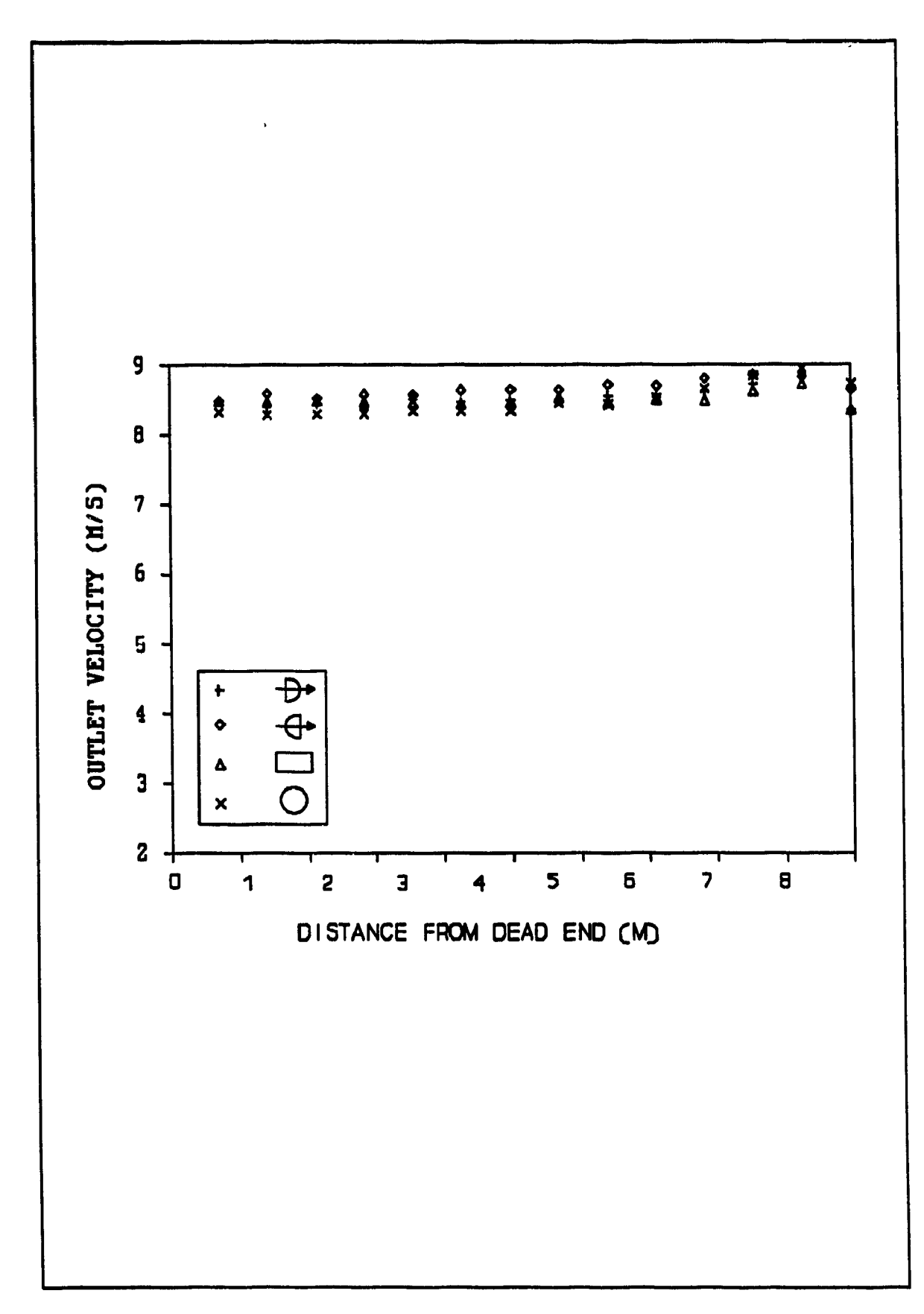


Figure 5.4 Outlet velocity curves for aperture ratio = 0.5

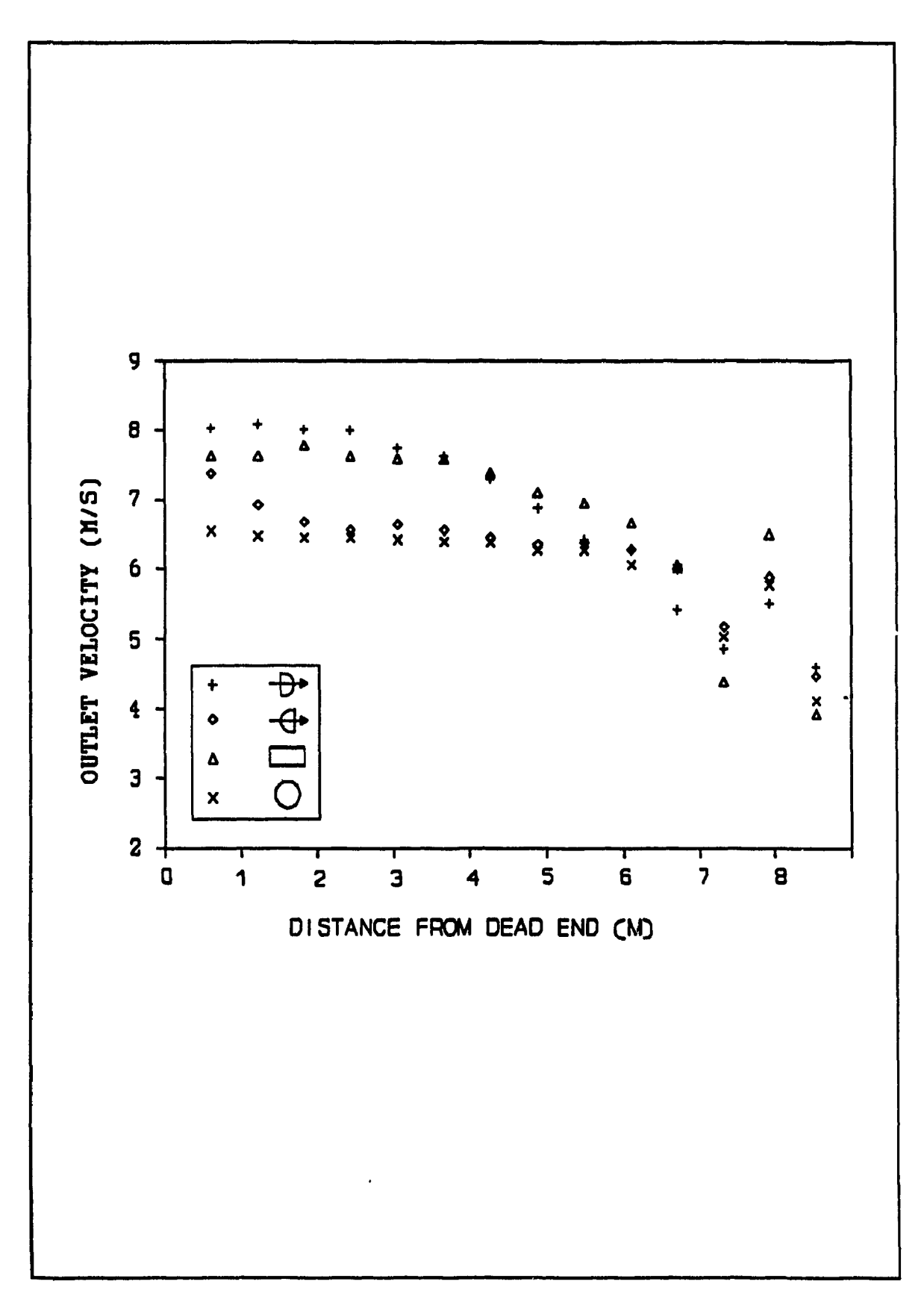


Figure 5.5 Outlet velocity curves for aperture ratio = 1.0

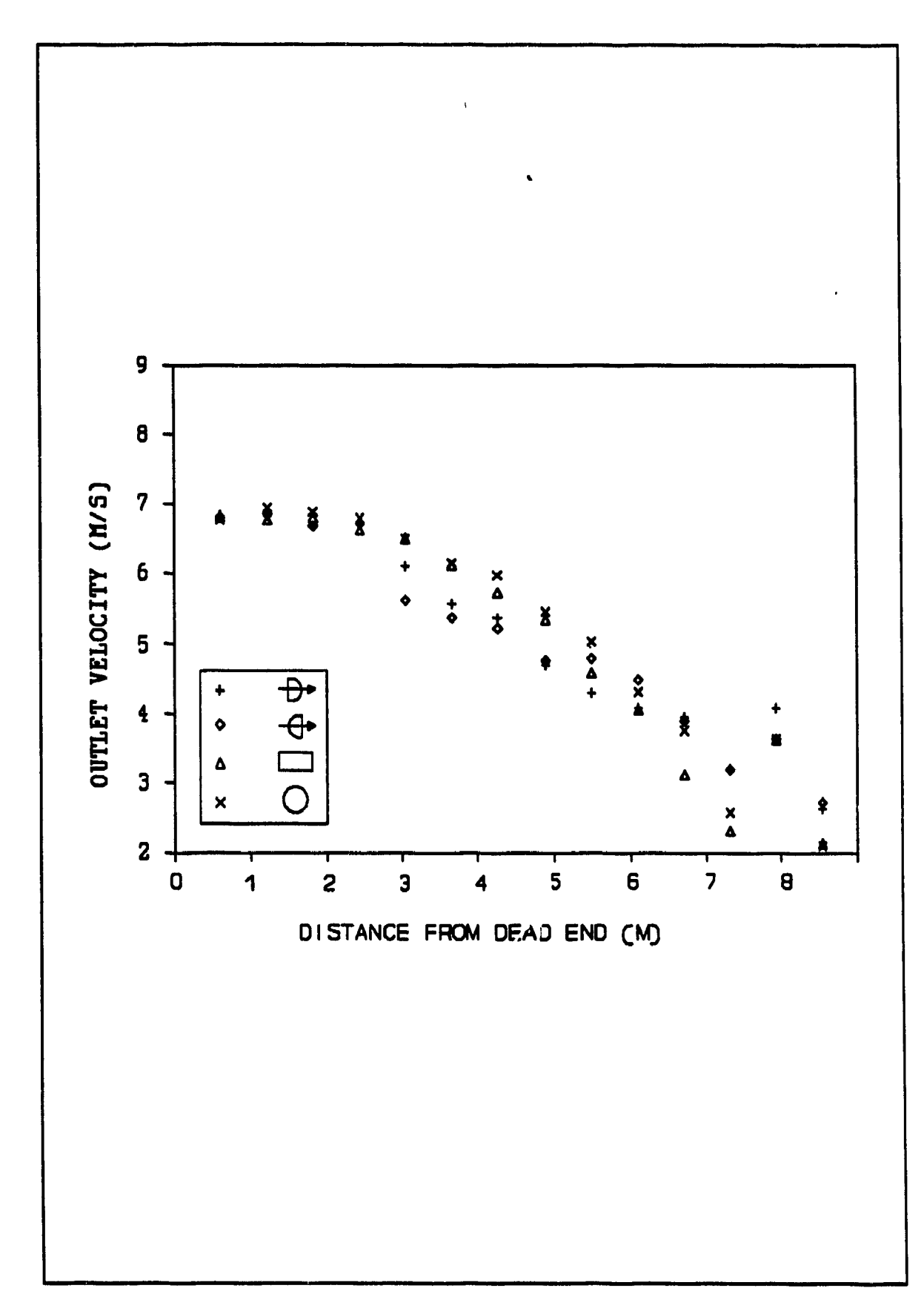


Figure 5.6 Outlet velocity curves for aperture ratio = 1.5

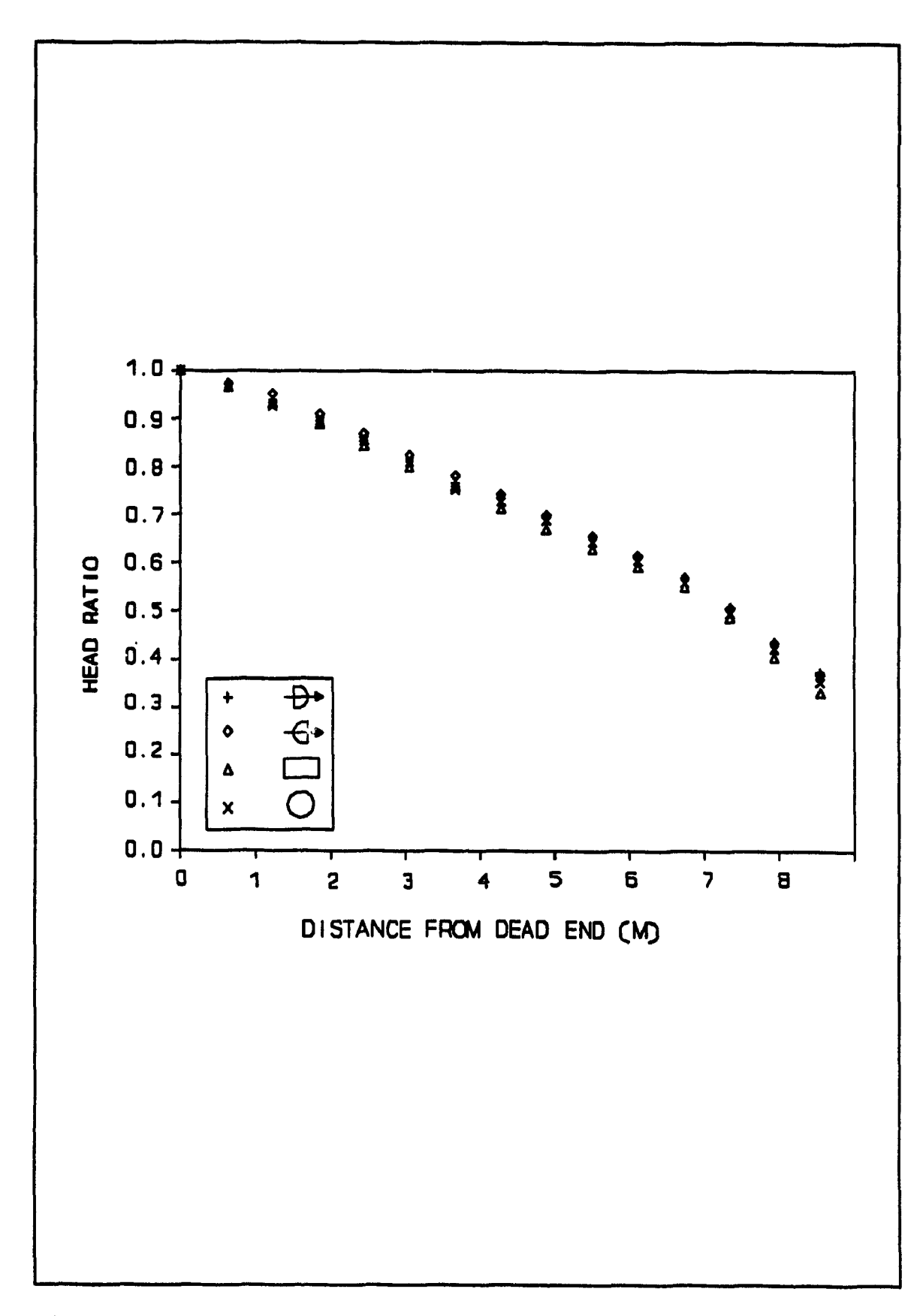


Figure 5.7 Head ratio curves for aperture ratio = 0.5

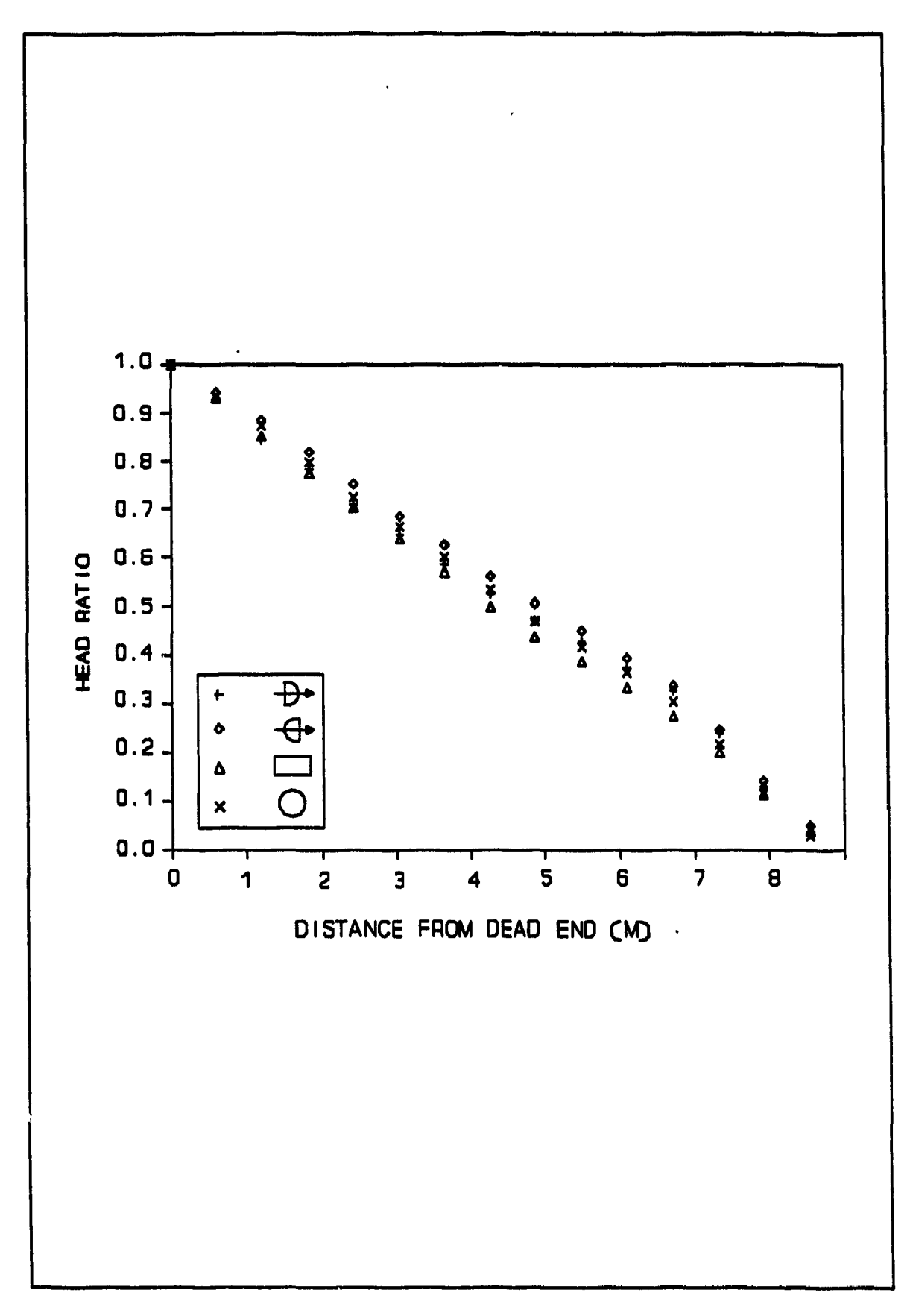


Figure 5.8 Head ratio curves for aperture ratio = 1.0

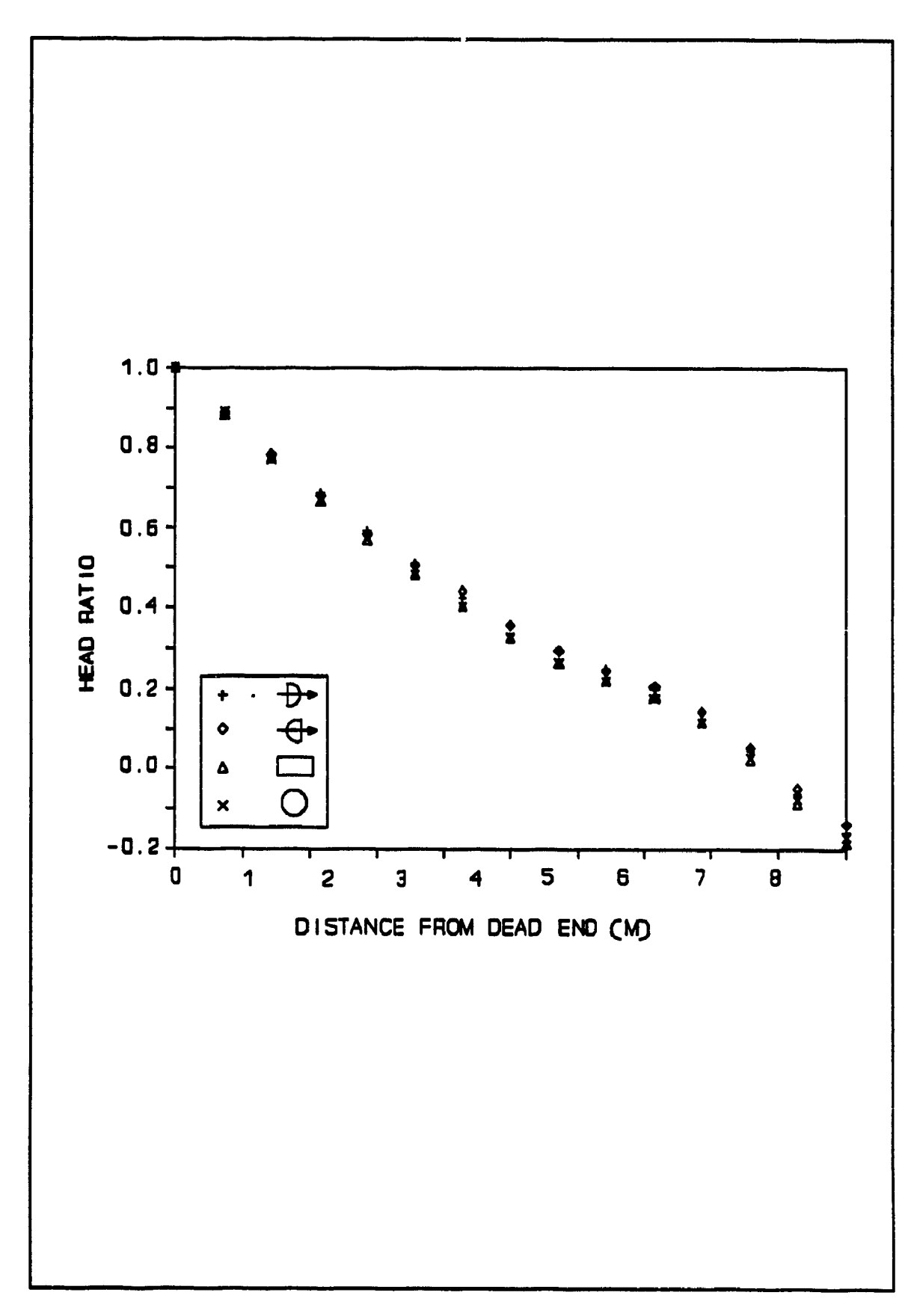


Figure 5.9 Head ratio curves for aperture ratio = 1.5

consistent with the findings of Haerter (1963) and Barrington and MacKinnon (1990). This suggests that in the mathematical modelling and design of ventilation ducts, it is necessary to account for the changing shape of the velocity profile with distance from the fan.

The outlet Reynolds number and the duct Reynolds number were each calculated from the data using equation 2.1. The outlet Reynolds number was calculated from the measured outlet velocities and was found to range from 10 000 to 65 000. The average duct velocity was calculated from the average outlet velocities. The duct Reynolds number ranged from 7 000 to 210 000. Since the Reynolds numbers were greater than 4000, fully turbulent flow may be assumed to have existed in the duct and at each outlet for every test.

The experimental data measured for the first 3 outlets after the fan is not consistent with the rest of the data. For each test there was an abrupt change in the static pressure and outlet velocity curves at a distance of about 7.5m from the dead end of the duct. This is probably due to unstable flow patterns caused by the reduction section and interference from the duct structural members. The steep slope of the pressure curves near the fan indicates that the duct was not flowing full up to the fourth outlet from the fan. This condition can be seen in plastic ducts where the first few metres closest to the fan are not fully inflated and are unstable (Carpenter, 1972). The duct static pressures below atmospheric pressure are an indication that the duct flow was not stable in the first few metres closest to the fan.

The measured discharge from the duct agreed with the measured intake at the fan to within 9% for all tests with an average difference of ±4.75% (Table 5.1). This is similar to the results of Brundrett and Vermes (1987).

**Table 5.1:**  $(Q_{in}-Q_{out})/Q_{in}*100\%$ 

APERTURE	SHAPE				
RATIO	1	2	3	4	
0.5	+7	+4	+8	+8	
1.0	+1	+3	+9	-1	
1.5	-4	-3	-6	-3	

The discharge coefficient was measured as the ratio of the average outlet velocity to the potential outlet velocity. As in Rawn et al. (1960), it was assumed that the entire duct energy head (static pressure head plus velocity head) generated a potential outlet velocity. The duct energy head was calculated from equation 3.8 and contained a correction factor to account for the variable duct velocity profile and momentum losses at the outlet. The calculated discharge coefficient values ranged from 0.193 to 1.254 with an average value of 0.845. The discharge coefficient data is presented in figures 5.10 to 5.12. Many of the measured values were greater than what has been reported in the literature. This can be explained by the inclusion of the kinetic energy and momentum correction factor in the duct energy head term to correct for variable velocity profiles. Because the outlet air comes from an area close to the wall of duct where the kinetic energy and momentum can be much less than average, the corrected energy term is less than if it had been calculated using mean velocity and the Bernoulli equation. Since the discharge coefficient is inversely related to the duct energy head, a smaller energy head

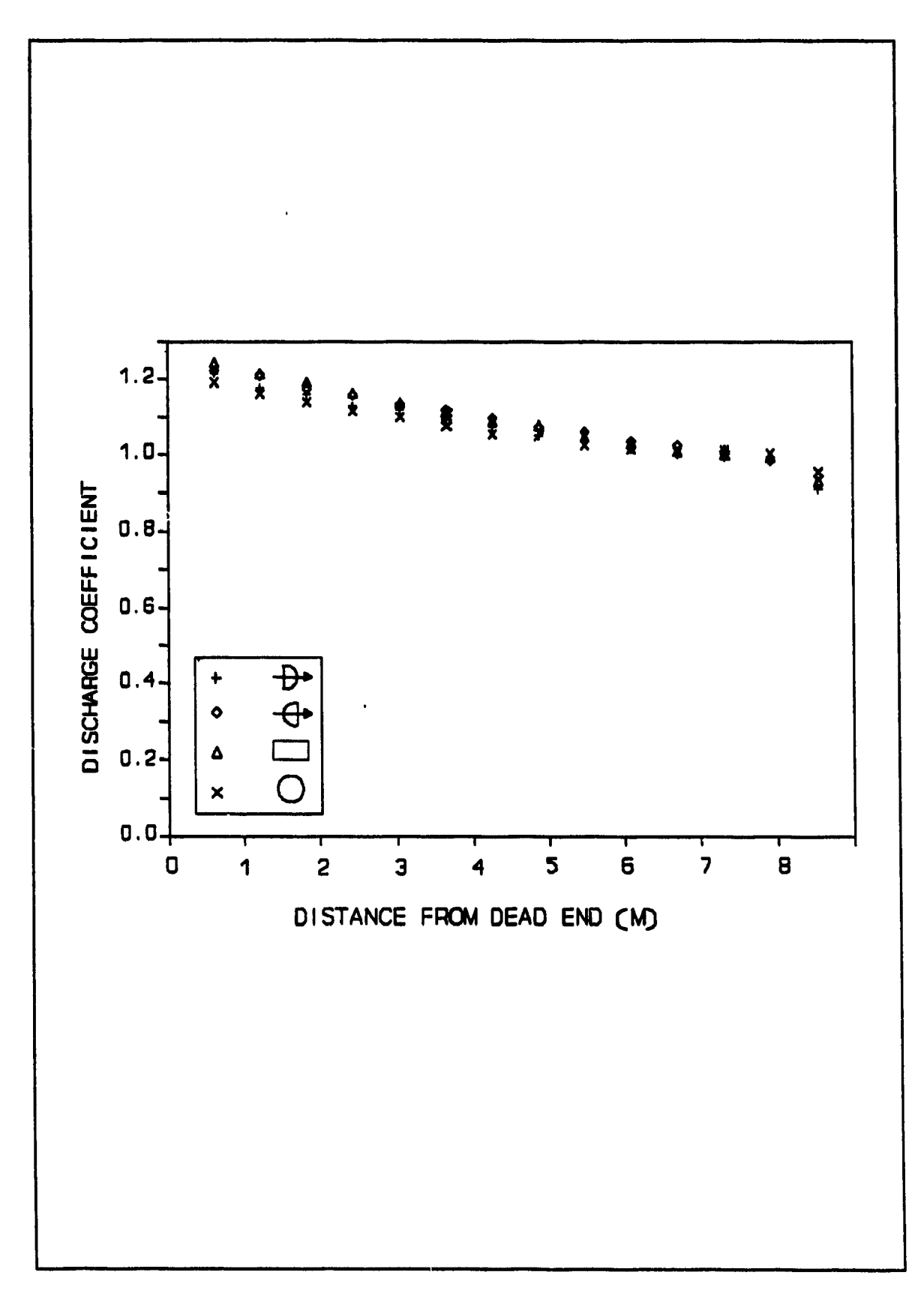


Figure 5.10 Discharge coefficients for aperture ratio = 0.5

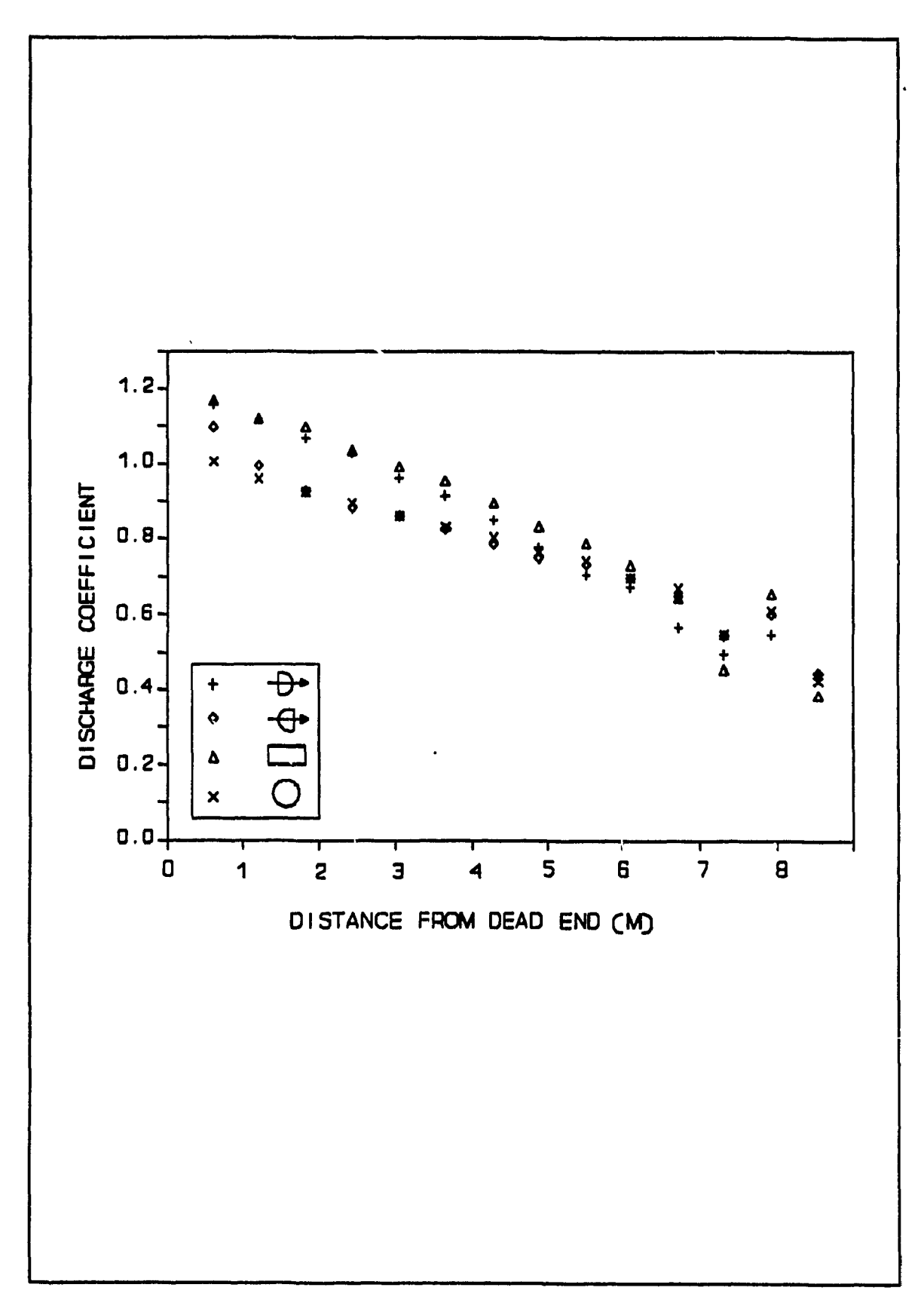


Figure 5.11 Discharge coefficients for aperture ratio = 1.0

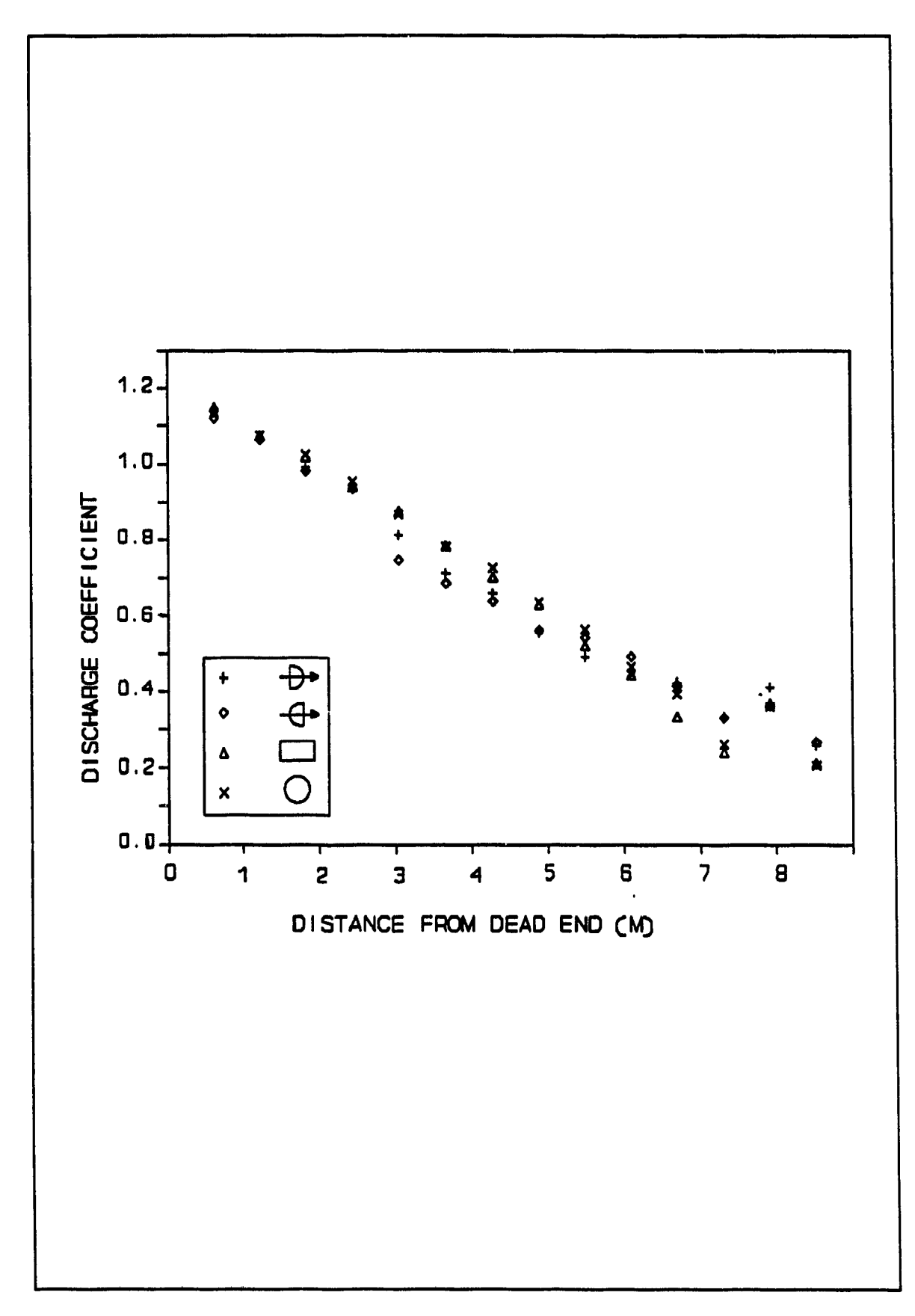


Figure 5.12 Discharge coefficients for aperture ratio = 1.5

value resulted in a larger discharge coefficient value.

The objectives of the experiment were to: 1) determine if outlet location along the length of the duct had an effect on the discharge coefficient, 2) determine if outlet geometry (shape and size) had an effect on the discharge coefficient, 3) determine the relationship between various duct operating characteristics and the discharge coefficient, and 4) develop and test an equation that will predict the discharge coefficients of ventilation duct outlets. To achieve objectives one and two, the experiment was performed with a split plot experimental design. A statistical analysis of the data was performed to test the significance of outlet location (distance from the fan), outlet size (aperture ratio), and outlet shape on the discharge coefficient. The results of the analysis are provided in appendix B and are summarized in table 5.2. The R<sup>2</sup> of the design was 0.991 with a coefficient of variation of 3.83%, thus the results of the analysis can be considered to be valid.

Table 5.2 Summary of the statistical analysis

SOURCE	SIGNIFICANCE	
Distance from the fan	**	
Outlet size	**	
Outlet shape	N.S.	
Size - Distance inveraction	**	

<sup>\*\*</sup> Significant at  $\alpha = 0.001$ 

N.S. Not significant

There was no significant difference between the discharge coefficient values for different shapes. This is also evident from figures 5.10 to 5.12. This may be explained by the high outlet Reynolds number. Since the outlet Reynolds number varied between 10 000 and 65 000 the viscous effects of the air had little influence compared to the inertia effects and thus outlet friction losses were minimal. Spikes and Pennington (1959) stated that the effect of outlet geometry is dependant on the friction losses caused by the outlet wall. Because the outlet wall area directly opposed to air flow was substantially different among shapes, it may be assumed that a wall thickness of 11mm has little effect on the discharge coefficient at outlet Reynolds number greater than 10 000.

The discharge coefficient was found to vary significantly with distance from the fan. Starting at the dead end of the duct, where the maximum discharge coefficient occurred for all tests, the discharge coefficient decreased at each outlet progressing towards the fan with the exception of the second outlet where the reduction section interfered with the air flow. The maximum difference between the aperture ratios occurred at the outlets closest to the fan. Progressing from the fan towards the dead end of the duct, the difference in discharge coefficient values among aperture ratios decreased until at the end of the duct the average discharge coefficient approached a common maximum value close to 1.20 for each test. These trends are similar to those found by Rawn et al. (1960) and Davis (1980).

There was a significant difference in discharge coefficient for each aperture ratio. For a given outlet, the discharge coefficient was generally highest at an aperture ratio of 0.5 and lowest at an aperture ratio of 1.5. The

size - distance interaction effect was significant, indicating that the effect of aperture ratio on the discharge coefficient changed with distance from the fan. Differences among aperture ratios were greatest near the fan, and were smallest at the dead end of the duct. The interaction effect is significant because regardless of outlet size, the conditions at the dead end of the duct approached that of a large reservoir, and the discharge coefficient approached a maximum value.

To achieve objective 3, to determine which operating characteristics affect the discharge coefficient, regression analyses of the data were performed to test for a simple linear relationship between; 1) discharge coefficient and head ratio (figures 5.13 to 5.15), 2) discharge coefficient and duct Reynolds number (DRe) (figures 5.16 to 5.18), 3) discharge coefficient and outlet Reynolds number (ORe)(figures 5.19 to 5.21), and 4) discharge coefficient and outlet discharge angle ( $\beta$ ). The correlation between head ratio and duct Reynolds number, and head ratio and outlet Reynolds number were also examined. The  $R^2$  of each analysis is presented in table 5.3.

Table 5.3 R<sup>2</sup> values for the linear regression analysis

ANALYSIS	0.5	1.0	1.5	ALL DATA
Cd vs. HR	0.827	0.849	0.936	0.872
Cd vs. DRe	0.777	0.854	0.902	0.905
Cd vs. ORe	0.007	0.733	0.879	0.260°
Cd vs. β	0.300	0.457	0.5 <b>79</b> °	0.584°
HR vs. DRe	0.881	0.970	0.933	0.890*
HR vs. ORe	0.001	0.564	0.771	0.260

<sup>\*</sup> Coefficient of variation > 20%

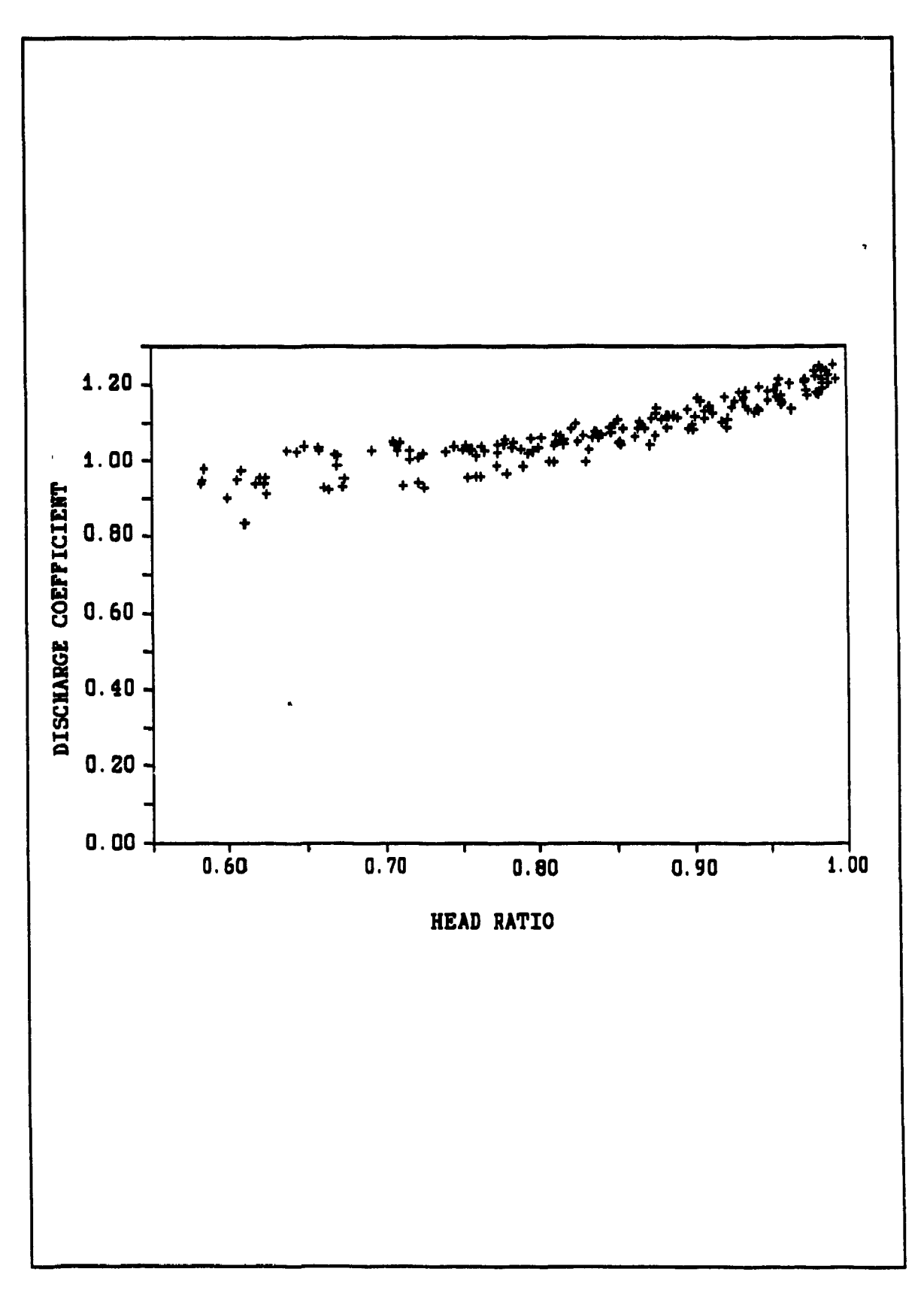


Figure 5.13 Discharge coefficient vs. head ratio:
Aperture ratio =0.5

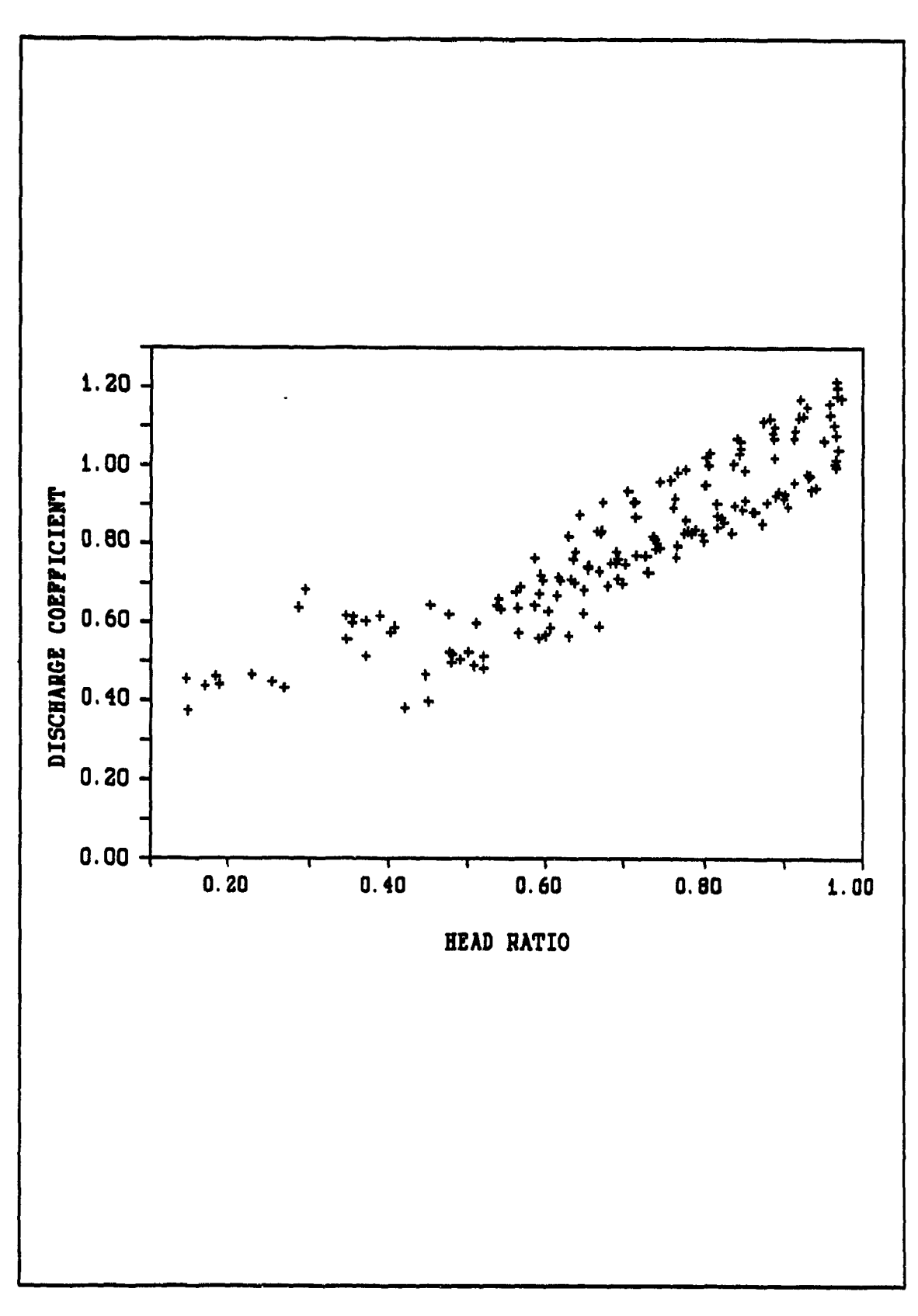


Figure 5.14 Discharge coefficient vs. head ratio:
Aperture ratio =1.0

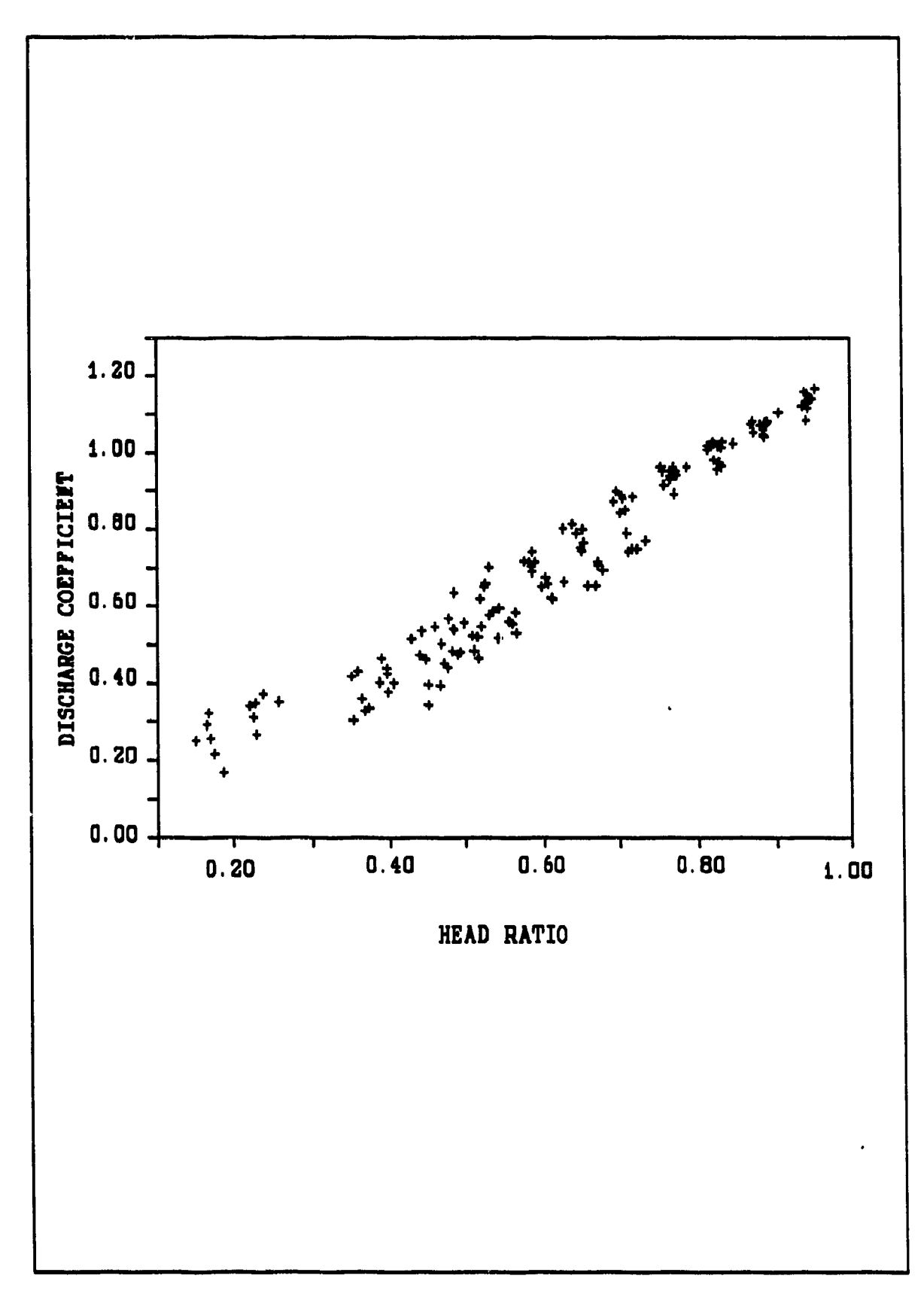


Figure 5.15 Discharge coefficient vs. head ratio:
Aperture ratio =1.5

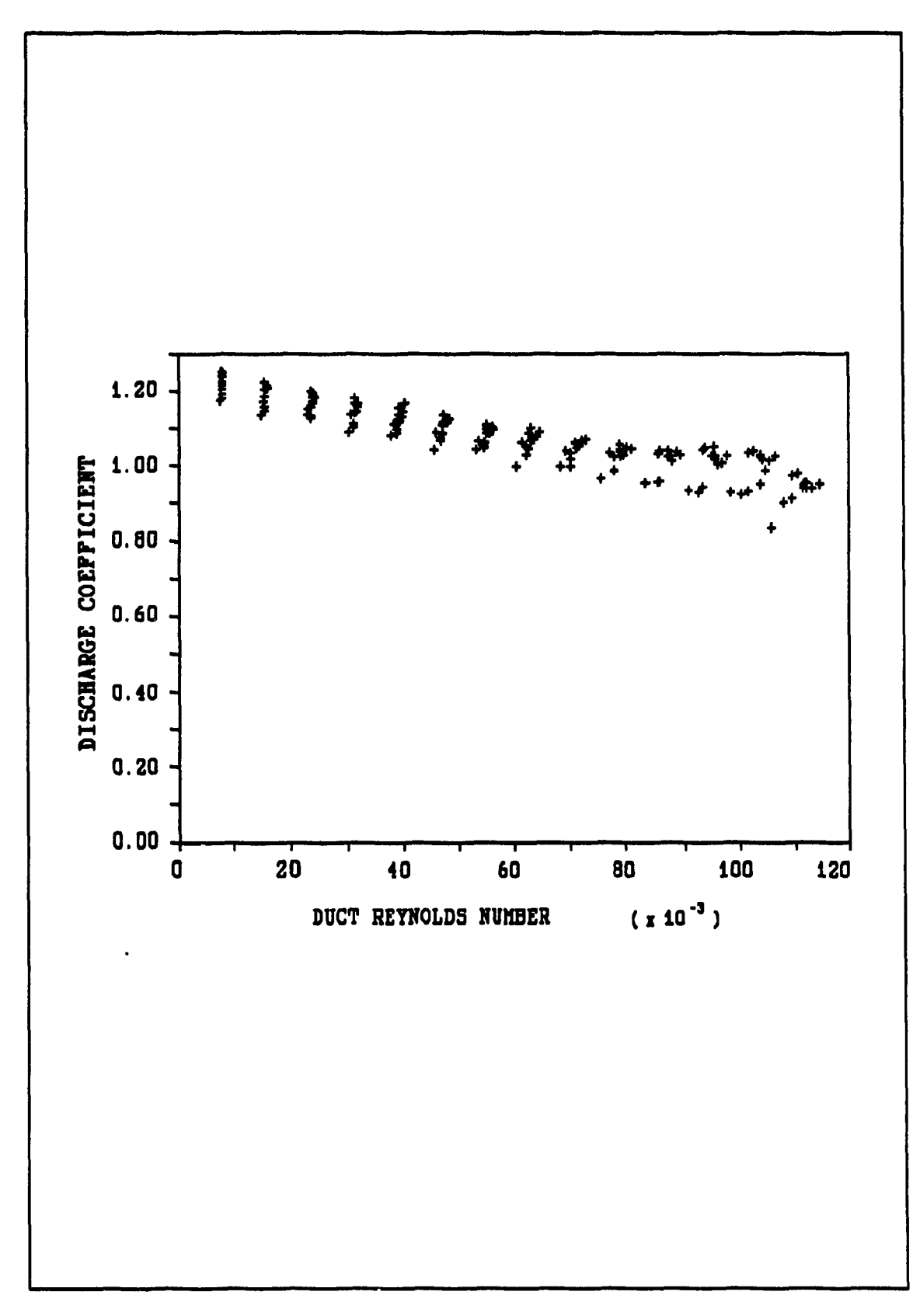


Figure 5.16 Discharge coefficient vs. duct Reynolds number:
Aperture ratio = 0.5

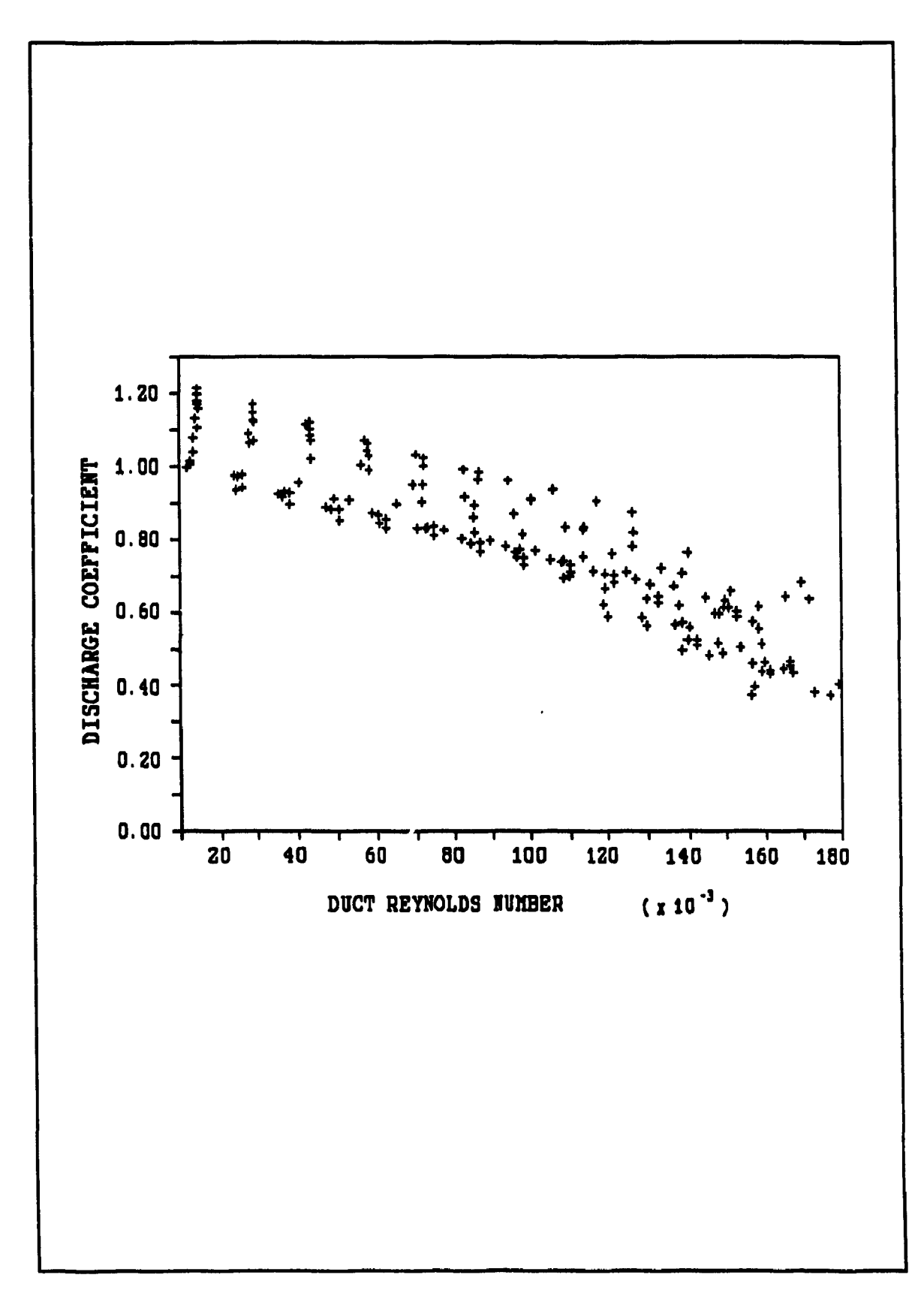


Figure 5.17 Discharge coefficient vs. duct Reynolds number:
Aperture ratio = 1.0

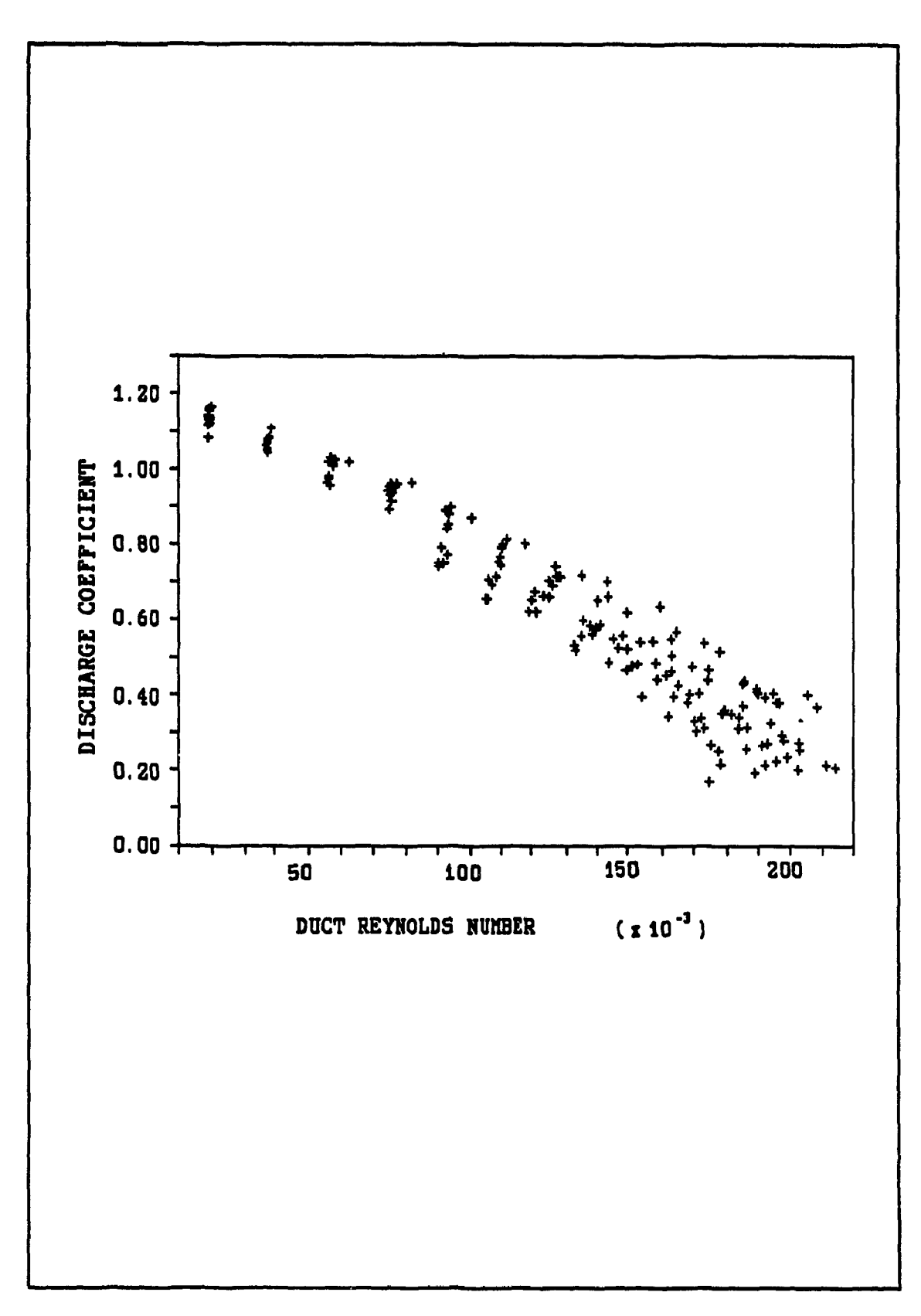


Figure 5.18 Discharge coefficient vs. duct Reynolds number:
Aperture ratio of 1.5

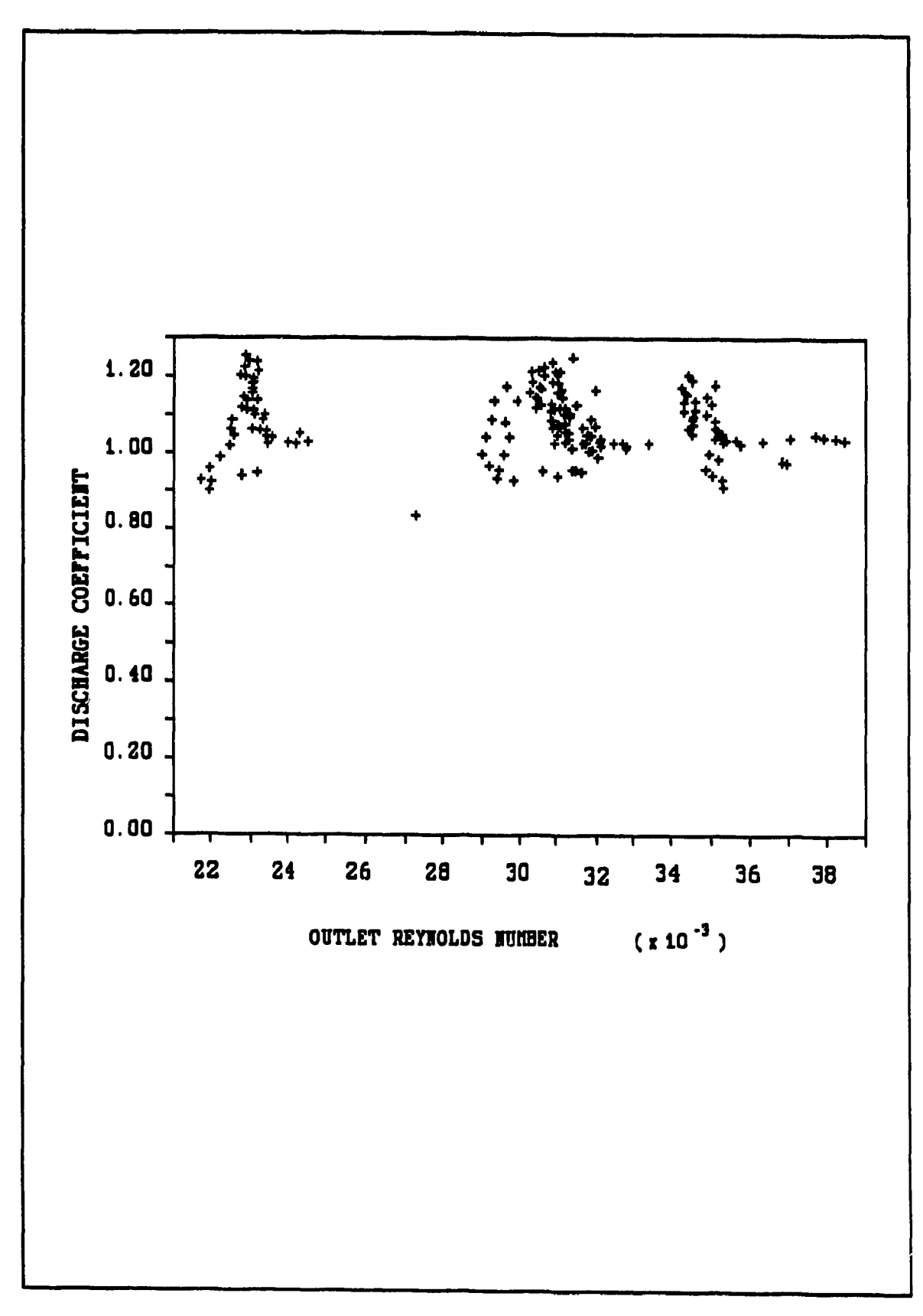


Figure 5.19 Discharge coefficient vs. outlet Re number:
Aperture ratio =0.5

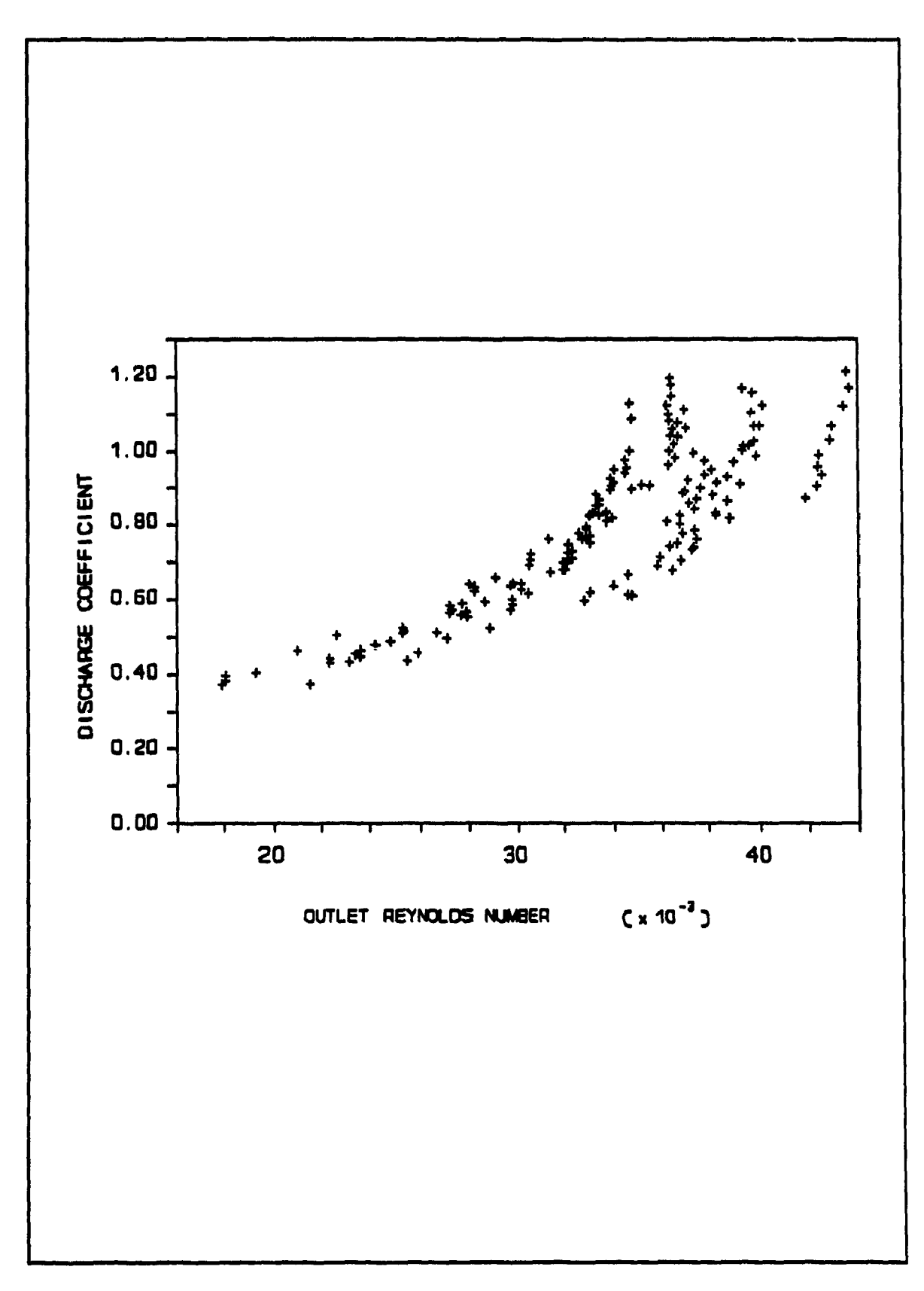


Figure 5.20 Discharge coefficient vs. outlet Re number:
Aperture Ratio =1.0

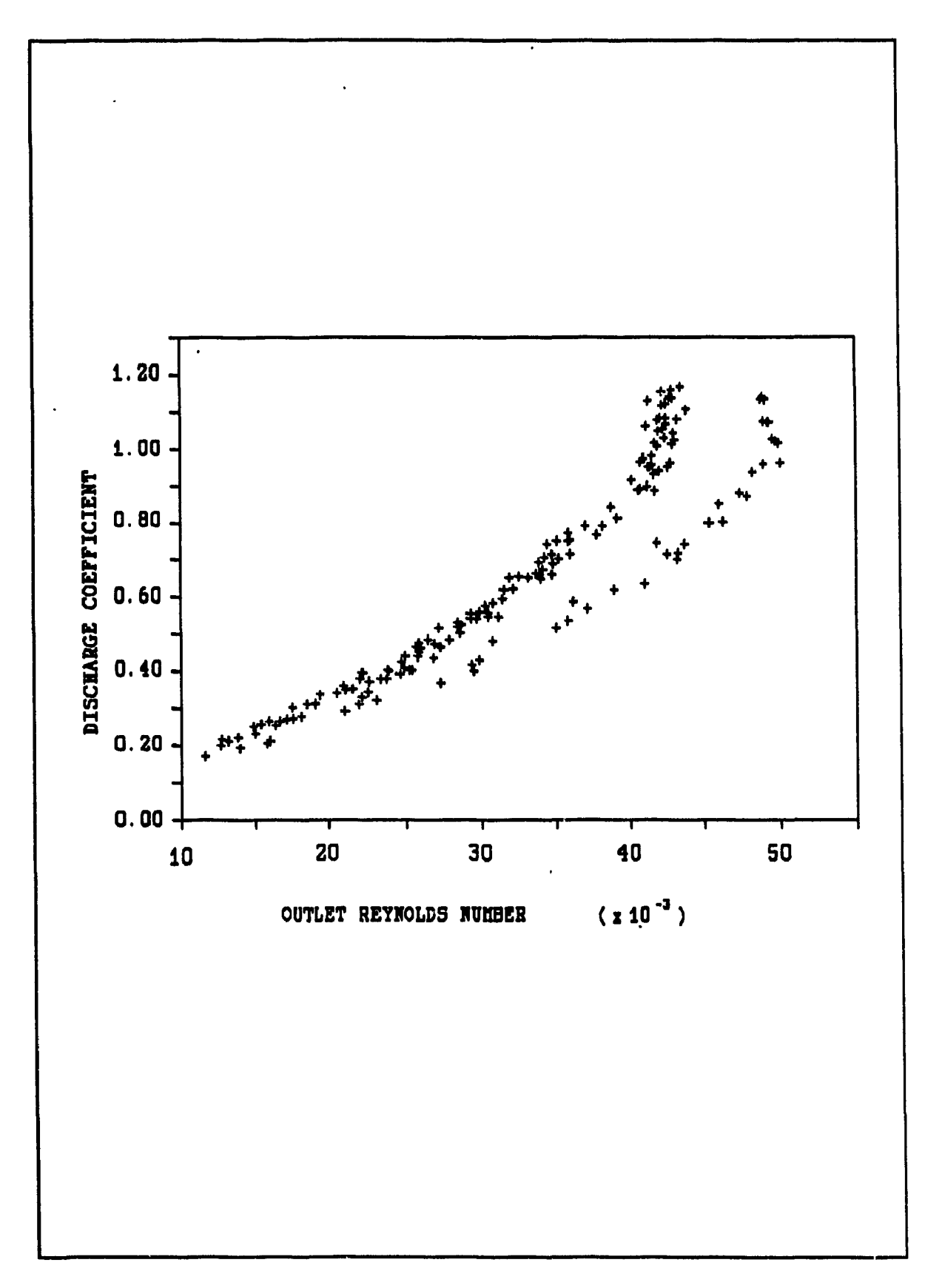


Figure 5.21 Discharge coefficient vs. outlet Re number:
Aperture Ratio =1.5

For all aperture ratios and shapes there is a high linear correlation between head ratio and discharge coefficient, duct Reynolds number and discharge coefficient, and duct Reynolds number and head ratio. There is no correlation between outlet Reynolds number and discharge coefficient at an aperture ratio of 0.5, a moderate relationship at an aperture ratio of 1.0, and a high linear relationship at an aperture ratio of 1.5. The correlation between outlet Reynolds number and head ratio also increased as aperture ratio increased. There is a correlation between outlet discharge angle and the discharge coefficient, but because of the high variation, it is not statistically significant. These analysis are consistent with the literature. Howland (1953) and Dittrich and Graves (in Bailey, 1975) stated that the duct velocity was the most important factor affecting discharge coefficient. However, the high linear correlation between head ratio and discharge coefficient indicates that it is not just duct velocity that is important but the relationship between duct velocity and duct pressure. The relationship between Reynolds number and discharge coefficient are consistent with the findings of Lichtarowitz et al. (1965) and Trengrouse (1970). They found that the discharge coefficient is a function of Reynolds number. However, since duct Reynolds number and outlet Reynolds number are each linearly related to the head ratio, the apparent effects of Reynolds number may be due to head ratio effects. Leonard and Kloseler (1938) suggested that the coefficient of contraction, and therefore the discharge coefficient, was dependant on the outlet discharge angle. The experimental data confirms that there is a correlation between the outlet discharge angle and the discharge coefficient, but this effect is not statistically significant.

The effects of size and aperture ratio on the discharge coefficient are directly related to the effect of head ratio on the discharge coefficient. Increasing aperture ratio, and increasing distance from the dead end of the duct had the same result; a decrease in the head ratio and the discharge coefficient (figure 5.22). At the dead end of the duct, where conditions in the duct resemble that of a large reservoir (constant pressure, no duct velocity, and head ratio of 1.0), there is very little difference between the discharge coefficients of each aperture ratio. Increasing aperture ratio or increasing distance from the back of the duct, resulted in the velocity head becoming a larger part of the total head, and decreasing the discharge coefficient. This is consistent with the conclusions of Enger and Levy (1929), Rawn et al. (1960), Bailey (1975) and Davis (1980) who stated that the discharge coefficient will exhibit a maximum value at the dead end, and will change as a function of the head ratio. From these analysis the apparent effects of aperture ratio and distance on discharge coefficient are due to the effects of head ratio.

To achieve the fourth objective, equation 3.16 was developed to predict discharge coefficient values and was tested against the experimental data. A comparison of the model to the data is presented in figure 5.23. The model predictions fitted the data very well for an aperture ratio of 0.5 with a maximum error of 2%. At an aperture ratio of 1.0 the model fit the data well except at the first and third outlets (8.4m and 7.2m from the dead end respectively) where the reduction section interfered with the duct flow. The maximum error at an aperture ratio of 1.0 was 5% at the middle of the duct. At an aperture ratio of 1.5 the model fits the data with a maximum error of 15%.

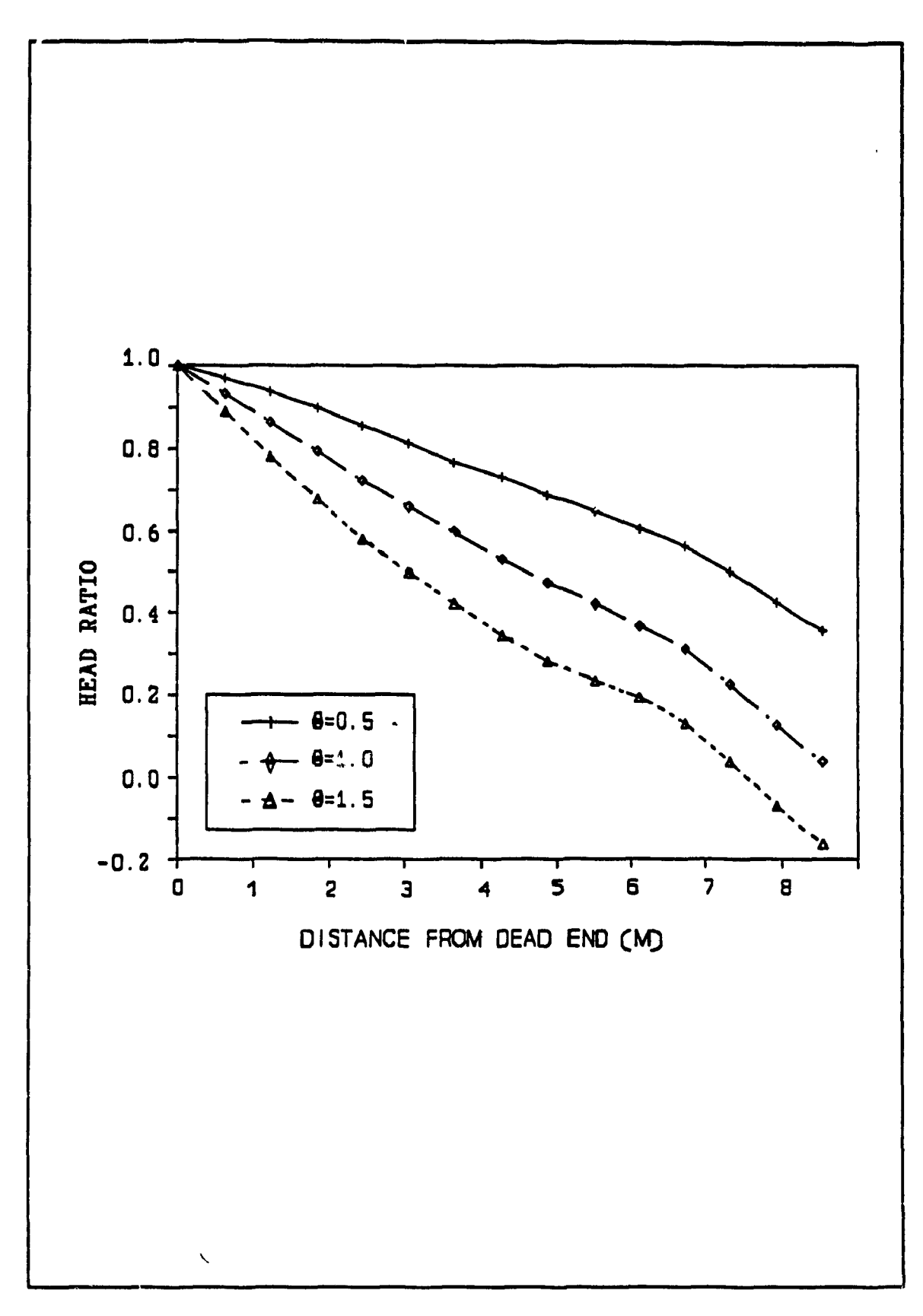


Figure 5.22 Head ratio curves (averaged over aperture ratio for all shapes)

The experimental data was used to evaluate the duct velocity and duct energy models of Barrington and MacKinnon (1990) to test their validity in the development of equation 3.16. The model of duct velocity was found to correlate very well with the data for aperture ratios of 0.5 and 1.0 but at an aperture ratio of 1.5 the model underestimates the duct velocity at the middle of the duct (figure 5.24). The maximum error for the aperture ratios of 0.5, 1.0, and 1.5 were in the order of 1%, 3%, and 12%, respectively. The model predictions for duct energy closely fit the data when considering the square root of the duct energy head (figure 5.25). The maximum error for all 3 aperture ratios was less than one percent. The error in equation 3.16 at aperture ratios of 1.0 and 1.5 is due to the error in the duct velocity model.

Several factors contributed to the experimental error. The anemometer operated within its indicated range of 0.1 m/s and 15 m/s throughout the experiment and was accurate to within ±3%. However, rotating the anemometer a small degree from the normal of the outlet plane resulted in an error greater than 3%. The turbulence of the air flow caused fluctuations in the anemometer readout and in the static pressure readings. The reduction section, and the structural members inside the duct caused disturbances in the air flow that affected the static pressure and duct velocity readings. Air leaks at the joints between the duct sections, and between the fan and the reduction section may account for a large proportion of the difference between inlet flow and outlet flow. The experimental error was close to what was found acceptable by Brundrett and Vermes (1937). The statistical analysis showed no significant difference between repetitions (appendix B).

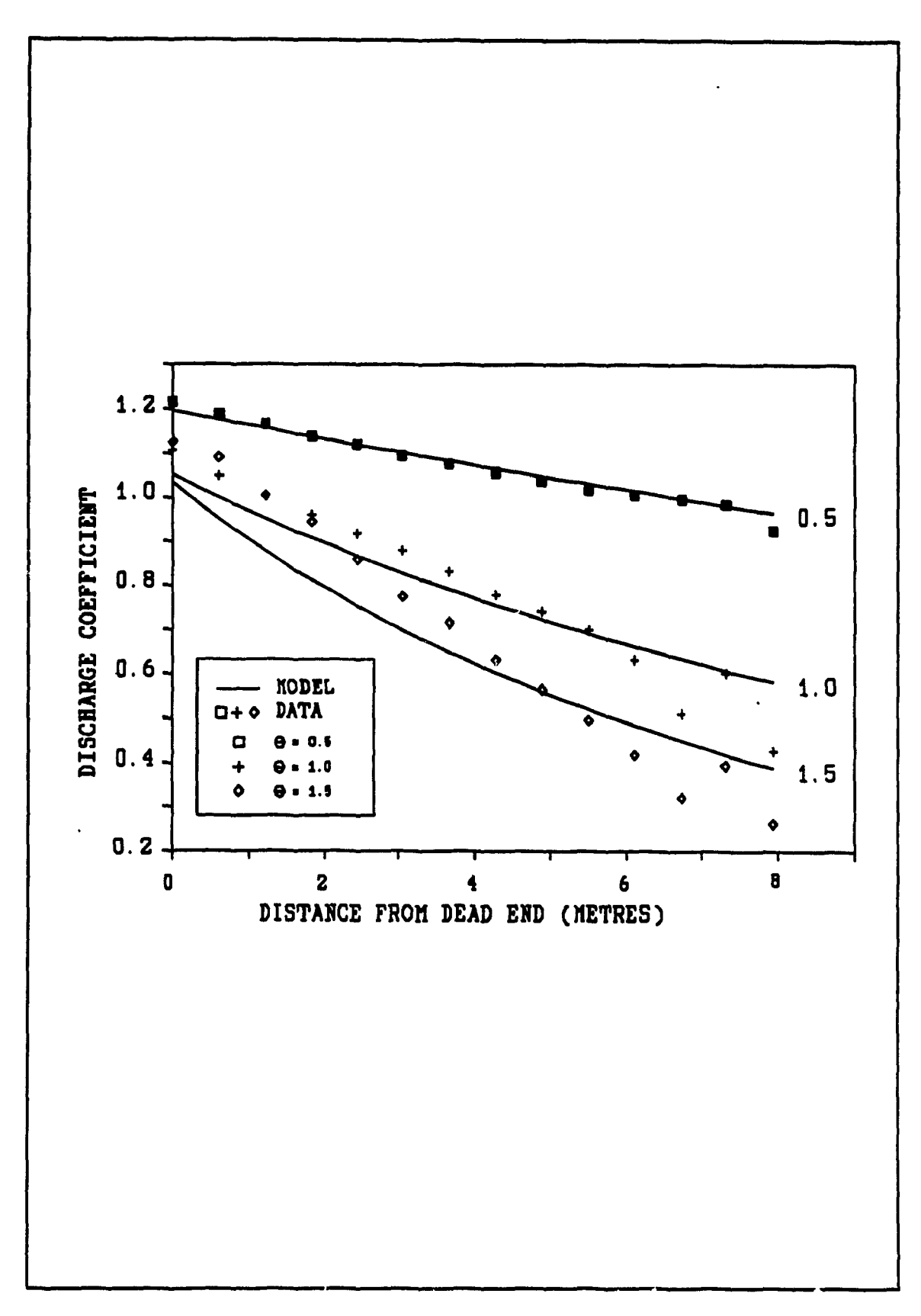


Figure 5.23 Equation 3.16 vs. the data

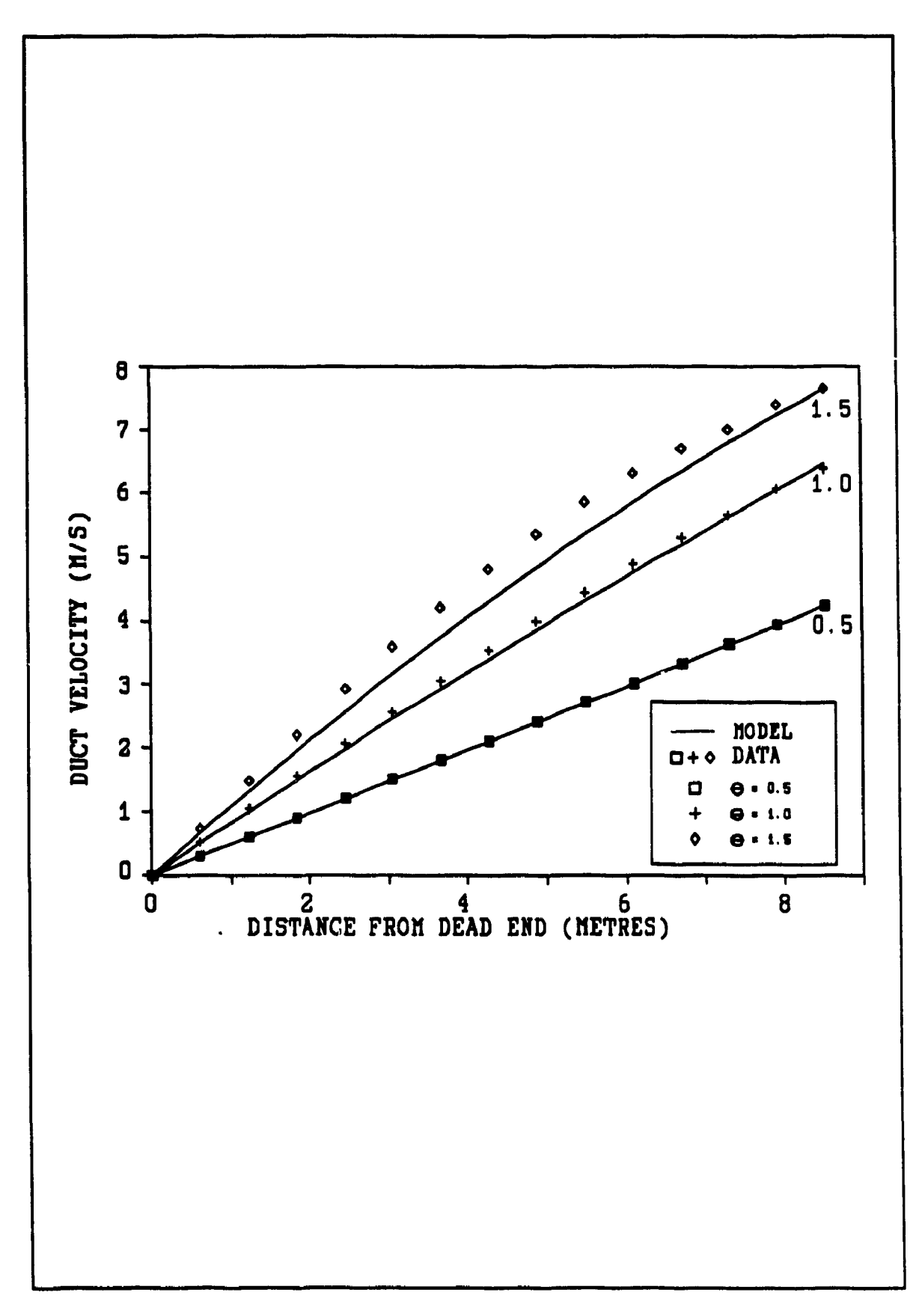


Figure 5.24 Equation 3.13 vs. the data

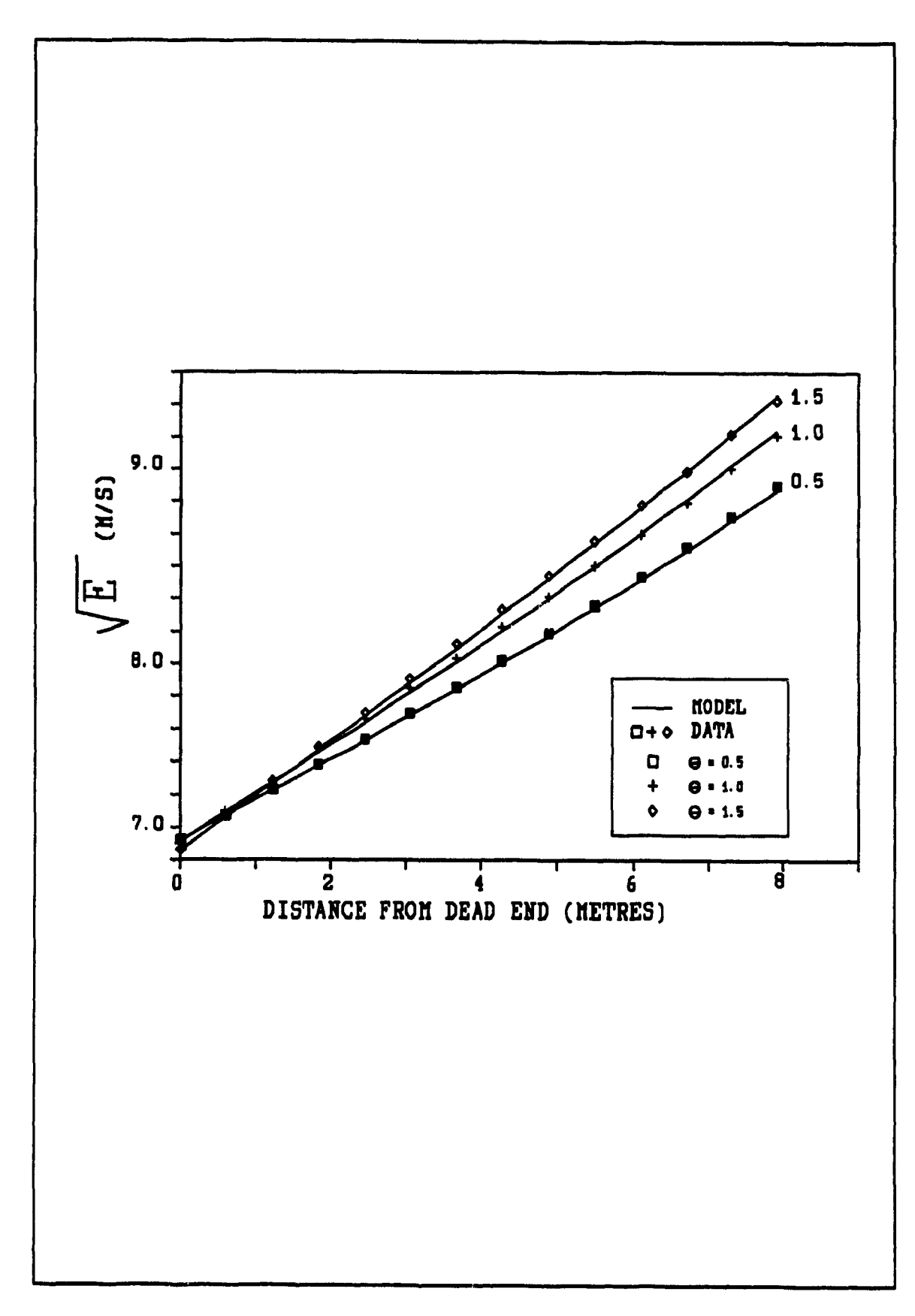


Figure 5.25 Equation 3.17 vs. the data

### **6.0 CONCLUSIONS**

The following conclusions are drawn from the project:

- 1) Outlet location along the length of the duct had a significant effect on the discharge coefficient of the ventilation duct outlets. To model the air displacement performance of ventilation ducts it is necessary to adjust the discharge coefficient as a function of duct length.
- 2) Outlet size had a significant effect on the discharge coefficient of the ventilation duct outlets. For a given distance from the fan, an increase in the aperture ratio of a duct will usually result in a lower discharge coefficient.
- 3) There is a significant interaction effect between outlet size and outlet distance from the fan. This indicates that the effect of outlet size on the discharge coefficient is dependant on the distance from the fan. Regardless of outlet size, the conditions at the dead end of the duct will approach that of a large reservoir, and the discharge coefficient will approach a maximum value.
- 4) The shape of the outlet had no significant effect on the discharge coefficient. At outlet Reynolds numbers of greater than 10 000 the friction forces are minimal and the effect of outlet shape is insignificant.
- 5) There is a linear relationship between the discharge coefficient and the head ratio, the discharge coefficient and the duct Reynolds number, and between the head ratio and the duct Reynolds number.

- 6) The apparent effects of outlet distance from the fan, outlet shape and duct Reynolds number, on the discharge coefficient are probably due to the effect of head ratio.
- 7) An equation was developed and tested to predict the discharge coefficient of ventilation ducts. The equation can estimate the discharge coefficient of ventilation ducts, with an aperture ratio of 1.0 or less, with a maximum error of less than 5 percent. Some error may be evident in the first few metres of the duct after the fan.

### 7.0 RECOMMENDATIONS FOR FURTHER RESEARCH

- 1) More research is required to compare the results of this experiment to other types of perforated ventilation ducts, and on wooden ducts of different lengths and diameters, to confirm that the findings are applicable to all types of ventilation ducts.
- 2) The experiments should be repeated in a wind tunnel using flow visualization techniques to confirm the assumptions of variable velocity profile and the loss of axial momentum at the outlet.

### 8.0 REFERENCES

- Albright, L.D. 1976. Airflow Through Hinged Baffle Slotted Inlets. Trans.

  ASAE 19(4): 728-732,735.
- Albright, L.D. 1978. Airflow Through Baffled, Centre Ceiling, Slotted Inlets.

  Trans. ASAE 21(5): 944-947.
- Allen, D. 1974. Air Distribution From Tapered Ducts. ASAE paper #74-6514.

  ASAE, St. Joseph, Michigan.
- American Society of Heating, Refrigerating, and Air Conditioning Engineers. 1985. Hand book of Fundamentals. ASHRAE, Atlanta Ga. pp. 13.14-13.16.
- Bailey, B.S. 1975. Fluid Flow In Perforated Pipes. Journal of Mech. Eng. Sci. 17(6): 338-347.
- Barrington, S.F. and I.R. MacKinnon. 1990. Air Distribution From Rectangular Wooden Ventilation Ducts. Trans ASAE, in press.
- Berlamont, J.A. and A. Van der Beken. 1973. Solutions for Lateral Outflow in Perforated Conduits. J. of the Hydraulics Division, ASCE No. 9: 1531-1549.
- Brundrett, E. and P.T. Vermes. 1987. Evaluation of Tube Diameter and Fan Induced Swirl In Polyethylene Ventilation Tubes. Trans. ASAE 30(4): 1131-1136.

- Bajura, R.A. 1971. A Model For Flow Distribution In Manifolds. ASME, J. of Eng. For Power 93: 7-13.
- Carpenter, G.A. 1972. The Design of Permeable Ducts and Their Application to The Ventilation of Livestock Buildings. J. Agric. Engng. Res. 17: 219-230.
- Cloud, H.A. and R.V. Morey. 1980. Distribution Duct Performance For Through Ventilation of Stored Potatoes. Trans. ASAE 23(5): 1213-1218.
- Davis, D.C. J.S. Romberger, C.A. Pettibone, S.C. Andeles, and H.J. Yeh.

  1980. Mathematical Model For Perforated Circular Ducts With

  Annular Corrugations. Trans. ASAE 19: 661-666.
- Denn, M.M. 1980. Process Fluid Mechanics. Prentice Hall Inc. Englewood Cliffs, N.J.
- Dow, W.M. and L.A. Shreveport. 1950. The Uniform Distribution of a Fluid Flowing Through a Perforated Pipe. Trans. ASME 71: 431-438.
- Enger, M.L., and M.I. Levy 1929. Pressures in Manifold Pipes. Proc.s A.W.W.A. 21: 659-667.
- Escobar, J. 1954. Discussion on McNowns paper "Mechanics of Manifold Flow". Trans. ASCE 119: 1119-1123.
- Esmay, M.L. and J.E. Dixon. 1986. Environmental Control For Agricultural

- Buildings. AVI Publishing Co. Westport Conn.
- French, J.A. 1972. Internal Hydraulics of Multiport Diffusers. J.W.C.P.F. 44(5):782-795.
- Haerter, A.A. 1963. Flow Distribution and Pressure Change Along Slotted or Branched Ducts. ASHRAE Trans. 69:124-137.
- Hellickson, M.A. and J.N. Walker. 1983. Ventilation of Agricultural Structures. ASAE St. Joseph, Michigan, USA.
- Howland, W.E. 1953. Design of Perforated Pipe for Uniformity of Discharge.

  Proc. 3rd Midwestern Conference on Fluid Mechanics. 687-701.
- Keller, J.D. 1949. The Manifold Problem. Trans. ASME 71: 77-85.
- Kincaid, D.C. and W.D. Kemper. 1982. Cablegation II: Simulation and Design of the Moving Plug Gated Irrigation System. Trans. ASAE 25: 388-395.
- Koestel, A. and C. Young. 1951. The Control of Airstreams From a Long Slot.

  Trans. A.S.H.V.E. 12: 497-418.
- Kreiss, R.F. 1945. Discussion on Soucek and Zelnicks paper "Lock Manifold Experiments". Trans. ASCE 110: 1389-1392.
- Leonard, J.J. 1987. High Pressure Ventilation Inlets for Animal Housing.

  CSAE paper #87-105. CSAE, Ottawa, Canada.

- Lichtarowitz, A., R.K. Duggins, and E.M. Markland. 1965. Discharge Coefficients for Incompressible Non Cavitating Flow Through Through Long Orifices. J. Mech. Eng. Sci. 7(2):210-219.
- McNown, J.S. 1954. Mechanics of Manifold Flow. Trans. ASCE 119: 1103-1142.
- Purser R.M.J. and D.J. Greig. 1967. Pressure Variations in Lateral Air Ducts. J. Agric. Engng. 12(3): 184-193.
- Olson, F.C.W. 1949. Flow Through a Pipe With a Porous Wall. Trans. ASME 71: 53-54.
- Ramamurthy, A.S. and M.G. Satish. 1987. Internal Hydraulics of Diffusers

  With Uniform Lateral Momentum Distribution. J. of the Env. Eng.

  Div., Proc.s ASCE 113(3): 449-463.
- Ramirez Guzman, H. and H. Manges. 1971. Uniform Flow From Irrigation Pipe. Trans ASAE 14:127-129.
- Rawn, A.M., F.R. Bowerman and H.B. Brooks. 1960. Diffusers For Disposal of Sewage in Seawater. J. of the Sanitary Eng. Div., Trans. ASCE 126: 344-388.
- Roberson, J.A., and C.T., Crowe. 1980. Engineering Fluid Mechanics. Hougton Mifflin Co., New Jersey.

- Saunders, D.D. and L.D. Albright. 1984. Airflow from Perforated Polyethylene Tubes. Trans. ASAE 23: 1144-1149.
- Smith, M.R. and T.E. Hazen. 1966. Similitude Study of Ventilation Inlet Configuration. ASAE Paper #66-915. ASAE, St. Josephs, Michigan.
- Smith, R.J., P.J Watts, and S.J. Mulder. 1986. Analysis and Design of Gated Irrigation Pipelines. Agrig. Water Manage. 12: 99-115.
- Smith, R.J. 1988. Energy Loss in Branching Flow and its Application to Irrigation Pipeline Design. J. Agric. engng. Res. 41: 181-189.
- Soucek, E. and E.W. Zelnick. 1945. Lock Manifold Experiments. Trans. ASCE 110: 1357-1400.
- Spikes, R.H. and G.A. Pennington. 1959. Discharge Coefficient of Small Submerged Orifices. Proc. Instn. Mech. Engrs. 173(25): 661-669.
- Statistical Analysis System Institute Inc. 1982. SAS Users Guide Statistics.

  SAS Institute, Raleigh, N.C.
- Steele, J.L. and G.C. Shove. 1969. Design Charts for Flow and Pressure Distribution in Perforated Air Ducts. Trans. ASAE 12: 220-224.
- Streeter and Wylie. 1981. Fluid Mechanics. MacGraw, Hill and Ryerson. New York, N.Y.
- Trengrouse, G.H. 1970. Steady Compressible Flow Through a Single row of Radial Holes in The Wall of a Pipeline. J. Mech. Eng. Sci. 12(4):

# 248-258.

Van't Woudt, B.D. 1964. Uniform Discharge From Multi Orificed Pipes.

Trans. ASAE 7(3): 352-355.

## 9.0 APPENDICES

# APPENDIX A.1: EXPERIMENTAL DATA

Appendix A contains a complete listing of the experimental data.

The data listed includes:

REP	=	repetition number
SHAPE	=	outlet shape;
		1 = half moon oriented with air flow
		2 = half moon oriented against air flow
		3 = rectangular
		4 = circular
A.R.	=	aperture ratio, dimensionless
X	=	outlet number (14= dead end, 1= fan end)
Vo	=	average outlet velocity, m/s
Vd	=	outlet velocity, m/s
P	=	duct static pressure, Pa
Cd	=	discharge coefficient, dimensionless
E	=	duct energy, m <sup>2</sup> /s <sup>2</sup>
K	=	duct energy correction factor, dimensionless
A	=	outlet discharge angle, degrees

REP	SHAPE	A.R.	х	Vo	Vd	P	CD	E	К	A
1	1	0.5	14 13 12 11 10 9 8 7 6 5 4 3 2	8.22 8.13 8.30 8.11 8.21 8.07 8.24 8.04 8.20 8.09 8.16 8.15 8.27 7.56	0.29 0.58 0.88 1.17 1.46 1.75 2.05 2.33 2.63 2.91 3.21 3.50 3.79 4.06	56.47 56.84 56.63 56.37 56.04 54.73 54.52 53.86 52.87 51.28 49.78 46.30 41.49 36.67	1.175 1.138 1.138 1.090 1.082 1.042 1.043 0.998 0.966 0.955 0.935 0.935	48.94 51.00 53.19 55.36 57.61 59.94 62.42 64.84 67.52 70.14 73.04 75.98 79.05 82.07	3.06 3.05 3.10	90 90 90 90 90 90 90 90 90
2	1	0.5	14 13 12 11 10 9 8 7 6 5 4 3 2	8.72 8.61 8.62 8.61 8.86 8.74 8.70 8.83 8.89 9.06 9.27 8.77	0.31 0.62 0.93 1.23 1.55 1.86 2.17 2.49 2.81 3.12 3.44 3.76 4.09 4.41	56.15 57.60 57.28 56.88 56.53 55.52 56.54 56.48 54.27 52.01 50.42 46.98 42.27 37.56	1.251 1.208 1.184 1.158 1.166 1.126 1.097 1.090 1.070 1.045 1.029 1.026 1.027 0.951	48.59 50.78 53.04 55.29 57.77 60.27 62.86 65.63 68.53 71.47 74.62 77.92 81.46 85.08	6.13 5.22 4.44 4.05 3.34 2.99 2.95 2.89 2.76 2.74 2.76	95 90 90 90 90 90 90 90 90 90
3	1	0.5	14 13 12 11 10 9 8 7 6 5 4 3 2	8.51 8.42 8.40 8.46 8.56 8.56 8.61 8.69 8.80 8.99 9.10 8.73	0.30 0.60 0.90 1.21 1.51 1.81 2.12 2.43 2.74 3.04 3.36 3.68 4.00 4.32	56.30 57.17 56.64 56.14 55.63 55.24 54.36 53.55 53.33 51.85 50.21 47.29 42.88 38.48	1.226 1.187 1.160 1.143 1.118 1.110 1.087 1.067 1.048 1.036 1.027 1.027 1.027	48.17 50.28 52.45 54.77 57.08 59.48 62.05 64.72 67.50 70.31 73.14 76.68 80.08 83.65	6.49 5.45 4.70 4.10 3.73 3.40 3.07 2.93 2.79 2.75 2.77	95 90 90 90 90 90 90 90 90 90

TABLE A.1 Data for shape 1, aperture ratio =0.5

REP	SHAPE	A.R.	Х	Vo	Vd	P	CD	E	K	A
1	1	1.0	14 13 12 11 10 9 8 7 6 5 4 3 2	8.54 8.56 8.51 8.42 8.40 9.32 8.31 8.34 8.30 8.21 5.47 4.75 5.82 4.64	0.55 1.11 1.66 2.19 2.69 3.17 3.63 4.07 4.50 4.87 5.26 5.60 6.02 6.35	55.58 54.65 53.88 52.44 51.74 51.07 49.49 47.45 45.74 43.80 40.11 31.78 20.11 8.45		49.55 53.60 57.78 62.02 66.26 70.57 74.94 79.38 83.97 88.25 92.96 97.42 102.94 107.81	6.54 4.67 3.82 3.20 2.79 2.56 2.40 2.26 2.18 2.15 2.26 2.38	90 90 85 85 80 80 80 75 75 75
2	1	1.0	14 13 12 11 10 9 8 7 6 5 4 3 2	7.78 7.86 7.79 7.79 7.47 7.26 6.48 5.99 5.53 5.34 5.36 4.96 5.48 4.60	0.56 1.12 1.67 2.23 2.76 3.28 3.75 4.17 4.57 4.95 5.33 5.69 6.08 6.41	49.87 49.77 50.00 48.73 47.54 45.76 43.32 41.56 39.81 36.58 33.75 25.65 14.11 2.57	1.158 1.123 1.070 1.029 0.951 0.893 0.772 0.693 0.622 0.385 0.572 0.516 0.555	49.01 53.01 57.32 61.65 66.16 70.53 74.72 78.96	4.07 3.36 2.89 2.61 2.45 2.31 2.19 2.15 2.10 2.19	90 90 90 85 85 85 85 85 85
3	1	1.0	14 13 12 11 10 9 8 7 6 5 4 3 2 1	7.77 7.84 7.75 7.81 7.38 7.29 7.10 6.30 5.44 5.34 5.43 4.86 5.24 4.55	0.55 1.12 1.67 2.23 2.75 3.27 3.78 4.23 4.62 5.00 5.39 5.74 6.11 6.44	55.38 53.78 54.72 54.08 53.11 51.57 49.62 47.51 45.78 42.61 39.65 30.72 17.27 3.81	0.989 0.903 0.862 0.813 0.700 0.589 0.564 0.559 0.488 0.513	53.70 57.89 62.38 66.79 71.47 76.33 80.95 85.26 89.72 94.51	4.41 3.48 2.98 2.66 2.45 2.31 2.21 2.17 2.12 2.23 2.41	90 90 90 85 85 85 85 85 85

TABLE A.2 Data for shape 1, aperture ratio =1.0

REP	SHAPE	A.R.	х	Vo	Vd	P	CD	E	K	A
1	1	1.5	14 13 12 11 10 9 8 7 6 5 4 3 2 1	6.75 6.71 6.52 6.72 6.67 6.05 5.44 4.79 4.11 4.14 3.80 3.38 3.93 2.39	0.72 1.44 2.14 2.86 3.58 4.22 4.81 5.32 5.76 6.20 6.61 6.97 7.39	38.86 38.52 37.72 36.37 35.07 31.99 29.82 27.06 25.03 22.15 15.92 5.90 -6.96 -19.82	1.118 1.048 0.964 0.941 0.886 0.767 0.661 0.561 0.465 0.453 0.403 0.349 0.393	36.48 41.00 45.74 50.99 56.67 62.20 67.74 73.02 78.03 83.38 88.77 94.00 100.14 104.97	7.90 4.29 3.12 2.53 2.14 2.00 1.85 1.78 1.72 1.69 1.73 1.83 1.94 2.08	90 90 90 80 80 75 70 70 70 70
2	1	1.5	14 13 12 11 10 9 8 7 6 5 4 3 2	6.96 7.02 6.89 6.84 5.74 5.57 5.39 4.93 4.56 4.13 3.29 4.03 2.80	0.75 1.50 2.24 2.97 3.58 4.18 4.76 5.29 5.77 6.71 7.06 7.49	38.80 39.38 38.70 37.37 35.76 32.75 31.34 27.13 24.54 21.56 16.53 5.46 -9.17 -23.81	1.167 1.107 1.025 0.962 0.771 0.716 0.664 0.584 0.521 0.504 0.440 0.341 0.404	35.57 40.24 45.22 50.53 55.38 60.54 65.92 71.29 76.61 82.48 88.18 93.35 99.63 104.93	5.76 3.30 2.58 2.20 2.00 1.90 1.76 1.74 1.69 1.64 1.65 1.78 1.91 2.06	90 90 90 90 85 85 85 85 85 80 80
3	1	1.5	14 13 12 11 10 9 8 7 6 5 4 3 2	6.79 6.76 6.64 6.66 5.93 5.11 5.31 4.37 4.24 3.55 3.94 2.96 4.30 2.73	0.73 1.45 2.16 2.88 3.51 4.06 4.63 5.10 5.55 5.93 6.35 7.13 7.42	38.34 37.51 37.08 35.81 34.02 31.82 28.42 25.06 23.85 20.93 16.24 5.56 -8.89	1.123 1.054 0.980 0.931 0.791 0.654 0.652 0.518 0.486 0.395 0.425 0.311 0.437 0.270	41.12 45.94 51.20 56.21 60.98 66.26 71.07 76.03 80.68 85.98 90.63	8.71 4.69 3.22 2.58 2.26 2.09 1.99 1.80 1.80 1.80 2.05 2.20	90 90 85 85 85 85 85 85 80 80

TABLE A.3 Data for shape 1, aperture ratio =1.5

REP	SHAPE	A.R.	х	Vo	Vd	Р	CD	E	K	A
1	2	0.5	14 13 12 11 10 9 8 7 6 5 4 3 2	8.58 8.60 8.58 8.64 8.65 8.63 8.70 8.67 8.81 8.81 8.90 8.84 9.09 8.61	0.31 0.61 0.92 1.23 1.54 1.85 2.16 2.47 2.78 3.09 3.41 3.73 4.05 4.36	55.96 56.92 57.08 57.01 56.68 55.93 54.65 53.97 52.13 51.43 48.19 43.23 38.27	1.238 1.215 1.186 1.168 1.145 1.118 1.104 1.077 1.068 1.049 1.037 1.008 1.014 0.940	48.01 50.12 52.36 54.67 57.06 59.54 62.12 64.80 67.59 70.50 73.63 76.90 80.32 83.82	3.36 3.16 2.93 2.83 2.65 2.64 2.70	90 90 90 85 85 85 85 85 85 85 85
2	2	0.5	14 13 12 11 10 9 8 7 6 5 4 3 2	8.47 8.63 8.49 8.63 8.57 8.67 8.63 8.69 8.67 8.71 8.82 8.88 8.61	0.30 0.61 0.91 1.22 1.53 1.84 2.14 2.45 2.76 3.07 3.38 3.70 4.02 4.32	56.18 57.42 57.66 57.42 56.80 56.14 55.93 55.42 54.16 53.10 51.20 47.66 43.32 38.98	1.217 1.213 1.169 1.163 1.130 1.119 1.085 1.069 1.054 1.030 1.013 1.004 0.989 0.939	48.42 50.61 52.79 55.11 57.51 59.99 62.49 65.18 67.97 70.89 73.93 77.20 80.62 84.01	7.41 5.72 4.88 4.35 3.90 3.47 3.16 3.00 2.83 2.74 2.74 2.75	90 90 90 90 90 85 85 85 85 85
3	2	0.5	14 13 12 11 10 9 8 7 6 5 4 3 2	8.41 8.51 8.48 8.45 8.49 8.59 8.66 8.67 8.59 8.78 8.70	0.30 0.60 0.91 1.21 1.51 1.82 2.13 2.44 2.75 3.05 3.37 3.68 3.99 4.30	56.55 57.98 57.45 56.96 56.67 56.30 55.46 54.53 53.90 53.50 51.40 48.21 43.40 38.60	1.215 1.204 1.173 1.145 1.127 1.116 1.102 1.074 1.057 1.026 1.026 1.019 0.952 0.955	47.88 49.99 52.23 54.46 56.77 59.24 61.80 64.47 67.25 70.06 73.17 76.33 79.64 83.10	4.64 5.25 4.78 4.19 3.72 3.43 3.20 2.95 2.74 2.67 2.67 2.73	90 90 90 90 90 85 85 85 85 85

TABLE A.4 Data for shape 2, aperture ratio =0.5

REP	SHAPE	A.R.	х	Vo	Vd	P	CD	E	K	A
1	2	1.0	14 13	7.70 7.27	0.55 1.07	49.08 50.82	1.171	43.20 46.72	7.61 3.81	90 90
			12	6.77	1.55	50.82	0.956	50.12	3.45	85
			11	6.65	2.03	49.55	0.907	53.70	3.01.	80
			10	6.81	2.51	48.24	0.898	57.48	2.74	80
			9	6.47	2.98	46.81	0.826	61.40	2.52	80
1			8	6.45	3.44	45.85	0.797	65.46	2.30	80
			7	6.42	3.90	44.12	0.769	69.77	2.17	80
			6	6.48	4.36	41.67	0.752	74.34	2.08	75
į			5	6.31	4.81	37.90	0.710	79.09	2.05	75
			4	6.17	5.25	35.38	0.673	84.05	1.98	75 75
			3	5.62	5.65	27.91	0.596	88.92	2.06	75 75
			2 1	5.98 4.64	6.08 6.41	17.13 6.35	0.616 0.466	94.37 99.13	2.17 2.28	75 75
				3.03	0.41	0.33	0.400	99.13	2.20	
2	2	1.0	14	7.20	0.51	54.14	1.040		10.91	90
			13	6.76	1.00	54.74	0.943	51.43	5.81	85
İ			12	6.64	1.47	53.89	0.896	54.92	4.63	85
			11	6.53	1.94	53.32	0.853	58.57	3.76	80
			10	6.55	2.41	51.95	0.829	62.41	3.29	80
			9 8	6.61 6.45	2.88 3.34	50.83 49.26	0.811 0.767	66.45 70.64	2.90 2.65	80 80
			7	6.31	3.79	47.68	0.707	74.97	2.45	75
İ			6	6.34	4.24	45.86	0.711	79.55	2.30	75
			5	6.27	4.69	42.71	0.682	84.40	2.22	75
			4	5.92	5.11	38.92	0.627	89.24	2.18	75
			3	4.95	5.47	30.58	0.511	93.77	2.28	75
			2	5.84	5.88	19.81	0.587	99.05	2.39	75
	·		1	4.39	6.20	9.05	0.431	103.68	2.50	70
3	2	1.0	14	7.20	0.51	49.99	1.079	44.53	11.05	90
			13	6.76	1.00	49.80	0.977	47.89	6.39	85
			12	6.64	1.47	49.88	0.927	51.25	4.48	85
			11	6.53	1.94	48.54	0.882	54.79	3.81	80
1			10	6.55	2.41	47.57	0.856	58.51	3.25	80
			9	6.61	2.88	46.66	0.837	62.44	2.84	80 75
			8 7	6.45 6.31	3.34 3.79	43.88 42.01	0.791 0.750	66.50 70.73	2.68 2.49	75 75
			6	6.34	4.24	40.36	0.731	75.20	2.49	75 75
			5	6.27	4.69	38.91	0.701	79.93	2.16	75 75
1			4	5.92	5.11	34.98	0.643	84.68	2.13	75
			3	4.95	5.47	26.92	0.524	89.12	2.23	70
			2	5.84	5.88	15.57	0.601	94.29		70
			1	4.39	6.20	4.21	0.442	98.85	2.48	70

TABLE A.5 Data for shape 2, aperture ratio =1.0

REP	SHAPE	A.R.	х	Vo	Vd	P	CD	E	ĸ	Α
1	2	1.5	14 13 12 11 10 9 8 7 6 5 4 3 2	6.73 6.87 6.64 6.52 5.74 5.21 5.15 4.56 4.88 4.47 3.81 3.45 4.07 2.89	7.30	40.86 40.72 39.32 37.83 36.09 33.98 30.69 28.09 25.80 23.55 17.71 7.65 -5.69 -19.03		38.49 43.26 48.19 53.43 58.38 63.30 68.48 73.52 79.17 84.84 90.21 95.51 101.82 107.15	8.56 4.38 3.28 2.66 2.34 2.14 2.04 1.94 1.76 1.79 1.89 2.00 2.12	85 80 80 80 75 70 70 70 70
2	2	1.5	14 13 12 11 10 9 8 7 6 5 4 3 2	6.83 6.79 6.55 6.83 5.52 5.49 5.47 5.03 4.88 4.99 4.38 3.61 3.79 2.61	0.73 1.46 2.16 2.89 3.48 4.07 4.66 5.20 5.72 6.26 6.72 7.11 7.52 7.80	38.35 38.01 37.04 35.54 33.60 32.66 28.65 25.24 22.85 20.84 16.11 6.48 -5.38 -17.24	1.140 1.067 0.974 0.961 0.743 0.708 0.675 0.597 0.557 0.548 0.465 0.372 0.378 0.254		7.44 4.13 3.07 2.50 2.24 1.99 1.92 1.85 1.76 1.67 1.67 1.76	90 90 85 85 80 75 75 75 75 75
3	2	1.5	14 13 12 11 10 9 8 7 6 5 4 3 2	6.86 6.92 6.86 6.81 5.62 5.42 5.05 4.69 4.59 3.99 3.52 2.54 3.05 2.66	0.74 1.48 2.21 2.94 3.54 4.12 4.67 5.17 5.66 6.09 6.46 6.74 7.35	38.91 37.86 36.48 35.22 33.78 29.83 26.79 23.94 22.21 16.44 5.80	0.952 0.751 0.694 0.621 0.556 0.524 0.441 0.378 0.266 0.311	40.93 45.88 51.22 56.02 61.02 66.16 71.24 76.59 81.76 86.69 91.02	6.89 3.88 2.93 2.41 2.13 1.94 1.89 1.77 1.71 1.75 1.90 2.07 2.22	90 90 85 85 80 80 75 75 75 75

TABLE A.6 Data for shape 2, aperture ratio =1.5

EP	SHAPE	A.R.	Х	Vo	Vd	P	CD	E	K	A
1	3	0.5	14	8.54	0.31	54.57	1.239	47.50		90
			13	8.56	0.61	54.39	1.215		11.48	90
			12	8.51	0.91	54.16	1.183	51.75	7.99	85
			11	8.42	1.22	53.76	1.145	54.05	6.22	85
			10	8.40	1.52	53.25	1.119	56.35	5.18	85
			9	8.32	1.81	53.12	1.086	58.66	4.39	85
			8	8.31	2.11	51.83	1.063	61.13	4.03	80
			7	8.34	2.41	51.08	1.045	63.70	3.64	80
			6	8.30	2.70	50.23	1.019	66.30	3.35	75
			5	8.21	3.00	49.58	0.988	69.08	3.08	75
			4	8.12	3.29	49.75	0.958	71.90	2.81	75
			3	8.03	3.57	47.30	0.929	74.75	2.77	75 70
			2	8.14	3.86	41.13	0.923	77.82	2.92	70
	<del></del>		1	8.12	4.15	34.97	0.902	81.02	3.01	70
2	3	0.5	14	8.44	0.30	53.31	1.254	45.28	9.51	90
			13	8.43	0.60	54.46	1.225	47.33	5.41	90
			12	8.44	0.90	54.14	1.200	49.44	5.34	90
			11	8.50	1.21	53.54	1.182	51.69	4.83	90
			10	8.50	1.51	52.97	1.157	53.94	4.30	85
			9	8.54	1.82	51.95	1.138	56.35		85
			8	8.51	2.12	51.11	1.110	58.78		85
			7	8.62	2.43	50.17	1.100	61.38		80
			6	8.50	2.73	49.49	1.062	64.01		80
			5	8.64	3.04	48.71	1.057	66.85		80
			4	8.70	3.35	47.45	1.041	69.81		80
			3	8.98	3.67	43.55	1.051	72.99		75
			2	8.95	3.99	37.95	1.024	76.32		75
			1	8.40	4.29	32.35	0.941	79.64	2.86	70
3	3	0.5	14	8.47	0.30	53.90	1.242	46.49	17.49	90
			13	8.39	0.60	54.06	1.204	48.57	9.77	90
		•	12	8.51	0.91	54.20	1.194	50.77	6.77	90
			11	8.50	1.21	53.78	1.168	52.98	5.57	90
			10	8.45	1.51	53.28	1.137	55.26	4.76	85
			9	8.45	1.81	52.72	1 113	57.62	4.18	85
			8	8.52	2.12	52.06	1.099	60.15		85
			7	8.60	2.42	50.87	1.086	62.70		80
			6	8.57	2.73	49.82	1.059	65.44		80
			5	8.63	3.04	49.08	1.044	68.30		80
			4	8.65	3.35	46.81	1.024	71.29		80
			3	8.86	3.66	42.68	1.027	74.41		75
			2	9.07	3.99	37.89	1.028	77.86		75
			1	8.54	4.29	33.10	0.948	81.20	2.91	70

TABLE A.7 Data for shape 3, aperture ratio =0.5

REP	SHAPE	A.R.	х	Vo	Vd	P	CD	E	K	A
1	3	1.0	14 13 12 11 10 9 8 7 6 5 4 3 2	7.38 7.40 7.88 7.38 7.25 7.24 7.12 7.07 6.68 6.52 5.97 4.83 6.35 3.85	0.53 1.06 1.62 2.15 2.66 3.18 3.69 4.19 4.67 5.14 5.56 5.91 6.36 6.64	47.08 46.38 45.80 45.31 44.66 43.49 41.13 39.06 37.17 34.60 30.23 26.45 23.97 21.51	1.130 1.089 1.113 1.003 0.951 0.916 0.869 0.762 0.721 0.641 0.505 0.644 0.382	42.64 46.19 50.15 54.11 58.16 62.53 67.09 71.86 76.76 81.88 86.85 91.43 97.27 101.70	12.11 6.71 4.57 3.54 2.96 2.60 2.41 2.24 2.10 2.01 1.99 1.99 1.91	90 90 85 85 80 75 70 65 65 55
2	3	1.0	14 13 12 11 10 9 8 7 6 5 4 3 2	7.75 7.76 7.73 7.77 7.78 7.79 7.48 7.04 7.23 6.97 6.20 4.47 6.33 4.11	0.55 1.11 1.66 2.22 2.77 3.33 3.86 4.36 4.88 5.38 5.82 6.14 6.59 6.89	47.11 47.40 46.74 45.87 44.80 44.08 41.34 39.14 37.04 34.25 31.09 22.18 9.67 -2.83	1.197 1.149 1.099 1.061 1.021 0.984 0.910 0.828 0.820 0.764 0.659 0.464 0.637 0.404	41.90 45.63 49.50 53.66 58.02 62.73 67.51 72.34 77.68 83.18 88.48 92.91 98.89 103.67	2.22 2.09 1.97 1.89 1.85 1.97 2.09	90 85 85 80 80 75 70 70 65 60 55
3	3	1.0	14 13 12 11 10 9 8 7 6 5 4 3 2	7.76 7.72 7.74 7.75 7.74 7.73 7.56 7.18 6.95 6.51 6.01 3.85 6.83 3.82	0.55 1.11 1.66 2.21 2.77 3.32 3.86 4.37 4.87 5.33 5.76 6.04 6.52 6.80	48.70 48.49 47.97 47.16 46.41 44.14 42.24 39.70 38.85 36.08 31.79 22.87 10.38 ~2.10		43.37 47.16 51.09 55.25 59.74 64.43 69.34 74.32 79.53 84.71 89.93 93.96 100.22 104.77	5.48 4.03 3.27 2.74 2.51 2.29 2.16 1.99 1.92 1.91 2.05 2.15	90 85 85 80 80 75 70 70 65 60 55

TABLE A.8 Data for shape 3, aperture ratio =1.0

REP	SHAPE	A.R.	х	Vo	Vd	P	CD	E	K	A
1	3	1.5	14 13 12 11 10 9 8 7 6 5 4 3 2	6.94 6.88 6.78 6.50 6.28 6.19 5.65 4.91 4.19 4.21 2.83 2.40 3.09 2.13			1.160 1.083 1.007 0.916 0.842 0.791 0.690 0.577 0.476 0.462 0.303 0.251 0.314 0.212	35.77 40.39 45.30 50.32 55.67 61.32 67.00 72.36 77.47 82.92 87.29 91.49 96.58 100.92	7.88 4.45 3.14 2.57 2.21 1.99 1.87 1.80 1.74 1.69 1.77 1.92 2.07 2.23	90 90 85 80 80 75 70 70 70
2	3	1.5	14 13 12 11 10 9 8 7 6 5 4 3 2	6.83 6.78 6.86 6.70 6.67 6.35 5.84 5.64 4.82 4.37 3.40 2.48 3.78 2.05				35.04 39.54 44.40 49.59 55.21 61.01 66.79 72.96 78.70 84.48 89.59 94.08 100.22 104.73	7.53 3.93 3.04 2.53 2.16 1.94 1.82 1.72 1.65 1.61 1.64 1.79 1.92 2.09	90 85 85 80 75 70 70 65 60 60 55
3	3	1.5	14 13 12 11 10 9 8 7 6 5 4 3 2	6.68 6.66 6.75 6.68 6.57 5.84 5.71 5.51 4.75 3.14 2.06 4.02 2.23	2.15 2.87 3.57 4.20 4.81 5.40 5.91 6.29 6.63 7.28	36.92 36.04 34.38 32.45 30.48 26.84 23.72 21.70 19.84 14.47	1.017 0.952 0.889 0.754 0.705 0.651 0.541 0.396 0.337 0.216 0.409	34.92 39.29 44.07 49.23 54.68 60.03 65.66 71.55 77.19 82.03 86.78 90.61 96.71	7.49 4.17 3.04 2.50 2.17 1.96 1.87 1.69 1.66 1.70 1.87 2.01	90 85 85 80 75 70 65 65 65 55

TABLE A.9 Data for shape 3, aperture ratio =1.5

REP	SHAPE	A.R.	х	Vo	Vd	P	CD	E	K	A
1	4	0.5	14 13 12 11 10 9 8 7 6 5 4 3 2	8.42 8.37 8.40 8.37 8.42 8.42 8.45 8.47 8.36 8.44 8.36 8.40 8.46	0.30 0.60 0.90 1.20 1.50 1.80 2.10 2.40 2.70 3.00 3.30 3.60 3.91 4.21	58.61 58.40 58.62 58.24 57.97 57.47 56.61 56.49 55.52 55.01 53.12 49.72 44.92 40.12	1.180 1.149 1.129 1.103 1.087 1.066 1.048 1.030 0.999 0.986 0.958 0.943 0.931	50.91 53.08 55.31 57.61 59.98 62.43 64.98 67.62 70.36 73.22 76.20 79.30 82.64 86.03	22.99 12.26 7.98 6.30 5.19 4.49 4.04 3.57 3.31 3.04 2.93 2.92 2.96 2.97	90 90 85 85 85 80 80 80 80
2	4	0.5	14 13 12 11 10 9 8 7 6 5 4 3 2	8.28 8.24 8.23 8.29 8.29 8.29 8.46 8.49 8.57 8.88 9.09 9.22 8.86	0.30 0.60 0.90 1.20 1.50 1.80 2.10 2.40 2.70 3.00 3.30 3.60 3.91 4.21	56.08 55.49 56.11 55.92 55.49 51.30 54.06 52.97 51.79 50.42 48.62 45.59 41.20 36.81	1.191 1.160 1.135 1.111 1.097 1.074 1.051 1.052 1.035 1.023 1.039 1.042 1.035 0.974		3.56 3.31 3.12 2.99 2.94 2.95	90 90 90 90 95 85 85 85 85 85
3	4	0.5	14 13 12 11 10 9 8 7 6 5 4 3 2	8.26 8.22 8.25 8.30 8.30 8.28 8.26 8.43 8.42 8.55 8.71 9.04 9.17 8.83	0.30 0.59 0.88 1.18 1.48 1.77 2.07 2.37 2.67 2.97 3.29 3.61 3.94 4.25	54.92 55.74 56.23 55.94 54.85 54.18 53.74 52.78 51.64 50.39 48.95 45.19 39.26 33.33	1.205 1.174 1.154 1.137 1.113 1.089 1.064 1.063 1.040 1.035 1.031 1.047 1.039 0.979	46.99 49.00 51.07 53.28 55.56 57.85 60.30 62.85 65.50 68.26 71.32 74.51 77.95 81.36	5.44 4.79 4.50 4.05 3.62 3.36 3.15 2.98 2.82 2.83 2.91	90 90 90 90 90 95 85 85 85 85

TABLE A.10 Data for shape 4, aperture ratio =0.5

REP	SHAPE	A.R.	Х	Vo	Vd	P	CD	E	K	A
1	4	1.0	14	6.33	0.45	45.20	0.997	40.29	12.97	90
			13	6.41	0.91	45.32	0.974	43.28	6.66	85
			12	6.29	1.36	43.88	0.924	46.34	5.29	80
			11	6.25	1.81	42.52	0.888	49.56	4.31	80
			10	6.35	2.26	42.25	0.873	52.94	3.47	80
			9	6.23	2.70	40.63	0.829	56.43	3.10	75
			8	6.23	3.15	39.33	0.803	60.20	2.76	75
			7	6.25	3.60	36.84	0.780	64.19	2.58	70
			6	6.16	4.04	35.23	0.745	68.34	2.39	70
			5	6.09	4.47	33.05	0.714	72.65	2.26	65
			4	6.07	4.90	29.98	0.691	77.23	2.18	65
			3	5.60	5.30	22.31	0.619	81.80	2.25	60
			2	5.56	5.70	13.01	0.597	86.65	2.33	60
			1	4.39	6.02	3.71	0.460	90.99	2.43	60
2	4	1.0	14	6.66	0.48	48.29	1.015	43.04	12.14	90
_	-	_,,	13	6.60	0.95	48.21	0.971	46.20	6.67	90
			12	6.56	1.42	47.26	0.932	49.50	5.02	85
			11	6.64	1.89	45.96	0.912	52.97	4.11	85
			10	6.34	2.34	44.99	0.844	56.47	3.47	80
			9	6.48	2.81	43.92	0.834	60.32	3.00	80
			8	6.57	3.28	41.62	0.819	64.39	2.76	80
			7	6.21	3.72	39.22	0.751	68.45	2.58	80
			6	6.33	4.17	37.39	0.742	72.84	2.40	75
			5	5.86	4.59	34.97	0.667	77.22	2.28	75
			4	5.76	5.00	31.31	0.637	81.77	2.23	70
			3	4.60	5.33	23.75	0.497	85.83	2.32	65
			2	5.86	5.75	13.12	0.614	90.97	2.42	65
			1	3.65	6.01	2.48	0.375	94.81	2.57	65
3	4	1.0	14	6.65	0.48	49.04	1.005	43.79	12.69	90
•	_		13			49.24				
			12	6.49	1.40	48.73	0.916	50.16	4.87	85
			11	6.46	1.86	47.72	0.883	53.58	3.99	85
			10	6.56	2.33	46.19	0.867	57.25	3.45	80
			9	6.40	2.79	45.01	0.829	61.04		80
			8	6.34	3.24	42.32	0.787	64.96		75
			7	6.35	3.70	39.92	0.763	69.20		75
			6	6.32	4.15	37.84	0.737	73.60		75
			5	6.24	4.59	35.83	0.706	78.17		75
			4	6.18	5.03	31.54	0.678	83.02		70
			3	4.89	5.38	23.97	0.523	87.30		70
			2	5.89	5.80	14.04	0.523	92.50		70
			1	4.31	6.11	4.12	0.612	96.89		70
			-		<b>√•</b> ±±	4 4 4 4	V. 4.00	20.03	2.50	70

TABLE A.11 Data for shape 4, aperture ratio =1.0

REP	SHAPE	A.R.	х	Vo	Vd	P	CD	E	K	A
1	4	1.5	14 13 12 11 10 9 8 7 6 5 4 3 2	6.79 6.82 6.89 6.67 6.36 6.28 5.89 5.02 4.26 3.12 3.07 1.61 3.04 1.93	0.73 1.46 2.20 2.91 3.59 4.26 4.90 5.43 5.89 6.22 6.55 6.72 7.05 7.26	38.02 37.56 36.67 35.23 33.61 31.52 28.16 25.22 22.88 20.00 14.16 3.82 -9.66 -23.14	1.134 1.073 1.023 0.938 0.851 0.800 0.716 0.587 0.481 0.343 0.329 0.169 0.311 0.193	35.83 40.38 45.36 50.52 55.89 61.63 67.58 73.06 78.31 82.70 87.32 90.63 95.65 99.71	7.78 4.26 3.06 2.50 2.16 1.95 1.84 1.77 1.71 1.76 1.94 2.09 2.26	90 85 85 75 75 60 60 55 55 55
2	4	1.5	14 13 12 11 10 9 8 7 6 5 4 3 2	6.75 8.83 6.92 6.93 6.61 6.40 6.00 5.15 4.86 4.07 2.92 3.79 2.18		22.38	0.367	35.34 41.28 46.34 51.82 57.55 63.61 69.75 75.87 82.18 88.67 94.82 100.02 106.55 111.50	7.41 3.63 2.70 2.27 2.01 1.86 1.59 1.55 1.57 1.69 1.82 1.97	85 85 80 80 75 75 75 75 75
3	4	1.5	14 13 12 11 10 9 8 7 6 5 4 3 2	6.76 6.77 6.86 6.77 6.54 5.79 6.06 5.99 5.68 4.97 4.14 3.19 4.08 2.21	7.89	37.45 36.83 35.04 32.95 30.86 27.36 24.64 22.42 20.00	0.744 0.743 0.701 0.637 0.536 0.431 0.323 0.400	60.59 66.57 72.97	6.75 4.02 2.91 2.43 2.13 1.95 1.84 1.72 1.62 1.56 1.59 1.71 1.83 1.98	85 85 80 80 75 75 75 75 75

TABLE A.12 Data for shape 4, aperture ratio =1.5

### APPENDIX A.2: EXPERIMENTAL DATA - MEAN VALUES

Data in tables A.13 to A.16 are averaged over 3 repetitions and are listed from X=14 to X=1.

Table A.13 Mean values of discharge coefficients, dimensionless

	APERTURE RATIO										
		0.5		L	1.	.0		1.5			
SHAPE					SH	APE		SHAPE			
1	2	3	4	1_	2	3	4	1	2	3	4
1.217 1.178 1.161 1.130 1.122 1.093 1.076 1.052 1.039	1.223 1.211 1.176 1.159 1.134 1.118 1.097 1.073 1.060	1.245 1.215 1.192 1.165 1.138 1.112 1.091 1.077 1.047	1.192 1.161 1.139 1.117 1.099 1.076 1.054 1.048 1.025	1.158 1.121 1.070 1.029 0.962 0.915 0.848 0.776 0.706	1.097 0.995 0.926 0.881 0.861 0.825 0.785 0.749 0.731	1.168 1.121 1.098 1.036 0.991 0.954 0.896 0.832 0.787 0.731	1.006 0.961 0.924 0.894 0.861 0.831 0.803 0.765 0.741	1.136 1.070 0.990 0.945 0.816 0.712 0.659 0.554 0.491	1.121 1.064 0.981 0.935 0.748 0.686 0.639 0.562 0.543	1.148 1.074 1.018 0.940 0.876 0.786 0.703 0.629 0.520	1.136 1.074 1.023 0.953 0.867 0.782 0.726 0.636 0.562
1.004 0.996 0.991 0.914	1.025 1.010 0.985 0.945	1.008 1.002 0.992 0.930	1.009 1.011 .1.002 0.955	0.566 0.495 0.547 0.446	0.648 0.544 0.601 0.446	0.645 0.455 0.654 0.386	0.669 0.546 0.608 0.424	0.423 0.334 0.411 0.259	0.415 0.330 0.364 0.266	0.333 0.241 0.367 0.211	0.393 0.261 0.359 0.204

Table A.14 Mean values of duct static pressure, Pa

APERTURE RATIO											
	(	).5			1.	0		1.5			
SHAPE					SH	APE			SH	APE	
1	2	3	4	1	2	3	4	1	2	3	4
55.80 56.31 57.20 56.85 56.46 56.07 55.16 55.14 54.63 53.49 51.71 50.14 46.86 42.21 37.57	55.22 56.23 57.44 57.40 57.13 56.72 56.12 55.71 54.87 54.01 52.91 51.34 48.02 43.32 38.62	53.25 53.93 54.30 54.17 53.69 53.17 52.60 51.67 50.71 49.85 49.12 48.00 44.51 38.99 33.47	55.99 56.54 56.54 56.99 56.70 56.10 54.32 54.80 52.98 51.94 50.23 46.83 41.79 36.75	53.19 53.61 52.73 52.87 51.75 50.80 49.47 47.48 45.51 43.78 41.00 37.84 29.38 17.16 4.94	50.13 51.07 51.79 51.32 50.47 49.25 48.10 46.33 44.60 42.63 39.84 36.43 28.47 17.50 6.54	46.99 47.63 47.42 46.84 46.11 45.29 43.90 41.57 39.30 37.69 34.98 31.04 23.83 14.67 5.53	47.24 47.51 47.59 46.62 45.40 44.48 43.19 41.09 38.66 36.82 34.62 30.94 23.34 13.39 3.44	38.31 38.67 38.47 37.83 36.52 34.95 32.19 29.86 26.42 24.47 21.55 16.23 5.64 -8.34	39.11 39.41 39.21 38.07 36.62 34.97 33.47 29.72 26.71 24.20 22.20 16.75 6.64 -6.58 -19.80		14.15 3.47

Table A.15 Mean values of outlet velocities, m/s

APERTURE RATIO											
	0	).5			1.0	0		1.5			
	SH	APE		SHAPE				SHAPE			
1	2	3	4	11	2	3	4	1	2	3	4
8.48	8.49	8.48	8.32	8.03	7.37	7.63	6.55	6.83	6.81	6.82	6.77
8.39	8.58	8.46	8.28	8.09	6.93	7.63	6.47	6.83	6.86	6.77	7.47
8.44	8.52	8.49	8.29	8.02	6.68	7.78	6.45	6.68	6.68	6.80	6.89
8.39	8.57	8.47	8.30	8.01	6.57	7.63	6.45	6.74	6.72	6.63	6.79
8.51	8.57	8.45	8.34	7.75	6.64	7.59	6.42	6.11	5.63	6.51	6.50
8.46	8.63	8.44	8.33	7.62	6.56	7.59	6.40	5.58	5.37	6.13	6.16
8.50	8.65	8.45	8.33	7.30	6.45	7.39	6.38	5.38	5.22	5.73	5.98
8.48	8.64	8.52	8.45	6.88	6.35	7.10	6.27	4.70	4.76	5.35	5.47
8.56	8.71	8.46	8.43	6.42	6.39	6.95	6.27	4.30	4.78	4.59	5.03
8.54	8.69	8.49	8.52	6.30	6.28	6.67	6.06	4.09	4.48	4.06	4.32
8.62	8.80	8.49	8.65	5.42	6.00	6.06	6.00	3.96	3.90	3.12	3.76
8.73	8.85	8.62	8.84	4.86	5.17	4.38	5.03	3.21	3.20	2.31	2.57
8.88	8.82	8.72	8.95	5.51	5.89	6.50	5.77	4.09	3.64	3.63	3.64
8.35	8.64	8.35	8.72	4.60	4.47	3.93	4.12	2.64	2.72	2.14	2.1

Table A.16 Mean values of duct velocity, m/s

				A	PERTU	RE RAT	IO				
J		0.5				1.0		1.5			
	SHAPE				SI	HAPE		SHAPE			
1	2	3	4	1	2	3	4	1	2	3	4
0.30 0.60 0.90 1.20 1.51 1.81 2.11 2.42 2.73 3.02 3.34 3.65 3.96	0.30 0.61 0.91 1.22 1.53 1.84 2.14 2.76 3.07 3.39 3.70 4.02	0.30 0.60 0.91 1.21 1.51 1.81 2.12 2.72 3.03 3.33 3.63 3.95	0.30 0.60 0.89 1.19 1.79 2.09 2.39 2.69 2.99 3.30 3.60 3.92	0.55 1.12 1.67 2.22 2.73 3.24 3.72 4.16 4.56 4.56 4.56 4.56 6.07 6.40	0.52 1.02 1.50 1.97 2.44 2.91 3.37 3.83 4.28 4.73 5.16 5.53 5.53 5.95 6.27	0.54 1.09 1.65 2.19 2.73 3.28 3.80 4.31 4.81 5.28 5.71 6.03 6.49 6.78	0.47 0.93 1.39 1.85 2.31 2.77 3.22 3.67 4.12 4.55 4.98 5.34 5.75	0.73 1.46 2.18 2.90 3.56 4.15 4.73 5.69 6.13 6.56 6.90 7.34	0.73 1.47 2.18 2.90 3.50 4.08 4.64 5.15 5.66 6.14 6.56 6.90 7.29	0.73 1.46 2.18 2.89 3.59 4.25 4.86 5.44 5.93 6.36 6.69 6.94 7.33	0.72 1.53 2.26 2.99 3.69 4.35 4.39 5.57 6.11 6.57 6.98 7.25 7.65

#### APPENDIX B: STATISTICAL ANALYSES

Appendix B contains a complete listing of the statistical analysis of the split plot experimental design. Tables B.1 lists the class level information. Table B.2 contains the results the analysis of variance (ANOVA) for the model. From table B.2; the effect of size is significant, the effect of outlet shape, repetition, and shape - size interaction is not significant. Two of the interaction effects listed in table B.2 are statistically significant but because the F values are several degrees of magnitude smaller than the F-values for SIZE and X they can be ignored.

Table B.1 ANALYSIS OF VARIANCE PROCEDURE: CLASS LEVEL INFORMATION

CLASS	LEVELS	VALUES
SHAPE	4	1 2 3 4
SIZE	3	1 0.5 1.5
DISTANCE (X)	14	1 2 3 4 5 6 7 8 9 10 11 12 13 14
REPETITION (REP)	3	1 2 3

Table B.2 Analysis of Variance (ANOVA)

SOURCE	DF	ANOVA SS	ANOVA MS	F VALUE	PR > F
REP	2	0.02196	0.01098	0.86	0.4364 <b>N.S.</b>
SHAPE	3	0.06226	0.02075	1.63	0.2116 N.S.
SIZE	2	14.64323	7.32162	574.34	0.0001 **
SHAPE*SIZE	6	0.14953	0.02492	1.95	0.1173 N.S.
ERROR 1	22	0.28045	0.01275		
X	13	18.04026	1.38771	1324.27	0.0 **
SHAPE*X	39	0.19133	0.00491	4.68	0.0001 1
SIZE*X	26	3,82630	0.14717	140.44	0.0 **
SHAPE*SIZE*X	78	0.27979	0.00359	3.42	0.0001 1
ERROR 2	312	0.32695	0.00105	3	, <del></del>
TOTAL	503	37.82165			

N.S. Not significant at  $\alpha=0.05$  or  $\alpha=0.01$ 

<sup>••</sup> Significant at  $\alpha = .001$ 

<sup>&#</sup>x27; Statistically significant but not significant compared to size and X.